Rho-Kinase Inhibition During Early Cardiac Development Causes Arrhythmogenic Right Ventricular Cardiomyopathy in Mice

Alia Ellawindy, Kimio Satoh, Shinichiro Sunamura, Nobuhiro Kikuchi, Kota Suzuki, Tatsuro Minami, Shohei Ikeda, Shinichi Tanaka, Toru Shimizu, Budbazar Enkhjargal, Satoshi Miyata, Yuhto Taguchi, Tetsuya Handoh, Kenta Kobayashi, Kazuto Kobayashi, Keiko Nakayama, Masahito Miura, Hiroaki Shimokawa

Objective—Arrhythmogenic right ventricular cardiomyopathy (ARVC) is characterized by fibrofatty changes of the right ventricle, ventricular arrhythmias, and sudden death. Though ARVC is currently regarded as a disease of the desmosome, desmosomal gene mutations have been identified only in half of ARVC patients, suggesting the involvement of other associated mechanisms. Rho-kinase signaling is involved in the regulation of intracellular transport and organizes cytoskeletal filaments, which supports desmosomal protein complex at the myocardial cell–cell junctions. Here, we explored whether inhibition of Rho-kinase signaling is involved in the pathogenesis of ARVC.

Approach and Results—Using 2 novel mouse models with SM22α- or αMHC-restricted overexpression of dominant-negative Rho-kinase, we show that mice with Rho-kinase inhibition in the developing heart (SM22α-restricted) spontaneously develop cardiac dilatation and dysfunction, myocardial fibrofatty changes, and ventricular arrhythmias, resulting in premature sudden death, phenotypes fulfilling the criteria of ARVC in humans. Rho-kinase inhibition in the developing heart results in the development of ARVC phenotypes in dominant-negative Rho-kinase mice through 3 mechanisms: (1) reduction of cardiac cell proliferation and ventricular wall thickness, (2) stimulation of the expression of the proadipogenic noncanonical Wnt ligand, Wnt5b, and the major adipogenic transcription factor, PPARγ (peroxisome proliferator activated receptor-γ), and inhibition of Wnt/β-catenin signaling, and (3) development of desmosomal abnormalities. These mechanisms lead to the development of cardiac dilatation and dysfunction, myocardial fibrofatty changes, and ventricular arrhythmias, ultimately resulting in sudden premature death in this ARVC mouse model.

Conclusions—This study demonstrates a novel crucial role of Rho-kinase inhibition during cardiac development in the pathogenesis of ARVC in mice. (***Arterioscler Thromb Vasc Biol*. 2015;35:2172-2184. DOI: 10.1161/ATVBAHA.115.305872.)**

Key Words: cytoskeletal filaments ■ desmosomes ■ myocardial fatty change ■ PPARγ ■ Rho-kinase ■ Wnt signaling pathway

Arrhythmogenic right ventricular cardiomyopathy (ARVC) is a genetically determined myocardial disease characterized by fibrofatty replacement, predominantly affecting the right ventricle (RV), ventricular arrhythmias, and an increased risk of sudden death, particularly in young people and athletes.[1] The recognition of biventricular or isolated left ventricular (LV) forms as part of the disease spectrum has recently encouraged the adoption of the broader term arrhythmogenic cardiomyopathy.[1] Mutations causing ARVC have been identified mostly in genes that encode the 5 major components of the cardiac desmosome: namely, desmoplakin, junction plakoglobin, plakophillin-2, desmoglein-2, and desmocollin-2.[2] Thus, ARVC is currently recognized as a disease of the desmosome.[2–4] Molecular genetic studies have identified mutations in ≥1 of the desmosomal genes in only approximately half of the ARVC patients,[4] suggesting that other

Received on: May 9, 2015; final version accepted on: August 17, 2015.

From the Department of Cardiovascular Medicine, Tohoku University Graduate School of Medicine, Sendai, Japan (A.E., K.S., S.S., N.K., K.S., T.M., S.I., S.T., T.S., B.E., S.M., H.S.); and Laboratory for Pharmacology, Pharmaceuticals Research Center, Asahi Kasei Pharma Corporation, Izunokuni, Japan (T.M., S.T.); Department of Clinical Physiology, Health Science, Tohoku University Graduate School of Medicine, Sendai, Japan (Y.T., T.H., M.M.); Department of Molecular Genetics, Institute of Biomedical Sciences, Fukushima Medical University School of Medicine, Fukushima, Japan (K.K., K.K.); and United Centers for Advanced Research and Translational Medicine, Core Center of Cancer Research, Division of Cell Proliferation, Tohoku University Graduate School of Medicine, Sendai, Japan (K.N.).

The online-only Data Supplement is available with this article at http://atvb.ahajournals.org/lookup/suppl/doi:10.1161/ATVBAHA.115.305872/-/DC1.

Correspondence to Hiroaki Shimokawa, MD, PhD, Professor and Chairman, Department of Cardiovascular Medicine, Tohoku University Graduate School of Medicine, Sendai 980-8574, Japan. E-mail shimo@cardio.med.tohoku.ac.jp

Nonstandard Abbreviations and Acronyms	
ARVC	arrhythmogenic right ventricular cardiomyopathy
DN-RhoK	dominant-negative Rho-kinase
E	embryonic day
LV	left ventricle
RV	right ventricle

disease-related genes may be involved. Despite considerable research advances for the genetic and molecular backgrounds of ARVC, the pathophysiological mechanisms still remain to be fully elucidated.[5]

Rho-kinase, the major downstream effector of the small GTPase Rho, is a protein kinase that has recently attracted much attention in the cardiovascular research field.[6] Abnormalities of the Rho/Rho-kinase pathway have been implicated in the pathogenesis of several cardiovascular disorders in human and animal studies.[7] Rho-kinase regulates a wide range of cellular functions, including actin cytoskeleton assembly, cell contractility, proliferation and differentiation, and gene expression.[8,9] In addition, the Rho/Rho-kinase system plays an important role in the regulation of adipogenesis.[10] Indeed, the Rho/Rho-kinase system has been shown to negatively regulate adipogenesis through interacting with Wnt signaling[11] and, in part, by controlling the expression of pro- and antiadipogenic Wnt genes.[10] Activation of canonical Wnt/β-catenin signaling is known to inhibit adipogenesis.[10] The less well-characterized noncanonical β-catenin–independent pathway, which involves activation of small G proteins and their downstream effectors, including the Rho/Rho-kinase system, plays a more complex role.[12] Interestingly, downregulated Wnt signaling has been recently implicated in the development of ARVC in mice.[13–15]

Because systemic Rho-kinase disruption in mice results in perinatal lethality, it has been difficult to examine the specific role of Rho-kinase in the cardiovascular system in mouse models. Thus, in the present study, we developed a novel mouse model in which Rho-kinase deficiency was targeted to the cardiovascular system during development. We here show that these Rho-kinase–deficient mice spontaneously develop unique phenotypes fulfilling the criteria of ARVC in humans associated with altered desmosome structure and aberrant Wnt signaling, indicating a novel and crucial role for Rho-kinase inhibition during development in the pathogenesis of ARVC in mice.

Materials and Methods

Materials and Methods are available in the online-only Data Supplement.

Results

Inhibition of Rho-Kinase Activity in the Developing Heart Through Overexpression of Dominant-Negative Rho-Kinase

To study the role of Rho-kinase inhibition in the cardiovascular system, we generated a novel mouse model in which dominant-negative Rho-kinase (DN-RhoK)[16] was overexpressed using the Cre-*loxP* system (Figure 1A and 1B). DN-RhoK consists of the carboxy-terminal fragment of Rho-kinase, which serves as an autoregulatory inhibitor of the amino-terminal kinase domain,[17] in which 2 point mutations were introduced to suppress Rho-binding activity.[16] DN-RhoK has been shown to inhibit intrinsic Rho-kinase activity when overexpressed in vivo.[18] Overexpression of DN-RhoK in our mouse model successfully reduced the activity of Rho-kinase in the embryonic day (E) 12.5 embryonic hearts (Figure 1C) and in the postnatal aortas (Figure 1D) of DN-RhoK mice compared with controls. We noted some sudden deaths of several pups before they were weaned at the age of 4 weeks. The breeding strategy used was expected to give rise to a 50% DN-RhoK offspring (Figure 1E). The genotype frequencies observed on E12.5 and until 1 week after birth in DN-RhoK mice were comparable to the expected frequency, indicating the absence of embryonic or neonatal lethality in DN-RhoK mice. However, the genotype frequency of DN-RhoK mice was reduced to 30% at 4 weeks of age (Figure 1E). The heart weight to body weight ratio and the ventricular weight to body weight ratio were both significantly higher in DN-RhoK mice compared with controls (Figure 1F). Systolic blood pressure was significantly lower in DN-RhoK mice compared with controls (Figure 1G). In addition, the aortas of DN-RhoK mice were thinner than those of controls (Figure 1H).

Crucial Role of Rho-Kinase in Cardiac Development

We first examined the sections of E12.5 embryos. Interestingly, we observed a marked thinning of the ventricular walls and interventricular septum of the hearts of DN-RhoK embryos (Figure 2A). Similar changes were noted in E14.5 hearts (Figure 2B) when the ventricular septation is normally completed and the heart has acquired the definite prenatal form.[19] To explore the mechanisms leading to ventricular thinning in DN-RhoK embryos, we examined cell proliferation and apoptosis in E12.5 hearts. TUNEL (TdT-mediated dUTP nick end labeling) assay showed a comparable extent of apoptosis between DN-RhoK and control hearts (Figure 2C). On the contrary, BrdU (bromodeoxyuridine) analysis showed a marked reduction in the number of proliferating cardiomyocytes in the ventricular walls and interventricular septum (both in compact layer and trabeculated layer) of DN-RhoK embryos and adult hearts compared with controls (Figure 2D).

Frequent Sudden Death and Cardiovascular Dysfunction in DN-RhoK Mice

Survival curves demonstrated a significantly higher mortality rate for DN-RhoK mice compared with controls, and by 1 year of follow-up, 34.6% of the DN-RhoK mice died suddenly (Figure 3A). Telemetry ECG recordings revealed significantly prolonged P-R intervals and QRS durations in DN-RhoK mice, suggesting the presence of cardiac conduction disturbances (Figure 3B). Interestingly, frequent spontaneous ventricular arrhythmias were detected in all the DN-RhoK mice examined, but not in the controls (Figure 3C). These spontaneous ventricular arrhythmias were evident as long frequent runs of ventricular extrasystoles characterized by widened QRS complexes with no apparent association with the P waves (Figure 3D). Interestingly, one of the DN-RhoK mice spontaneously

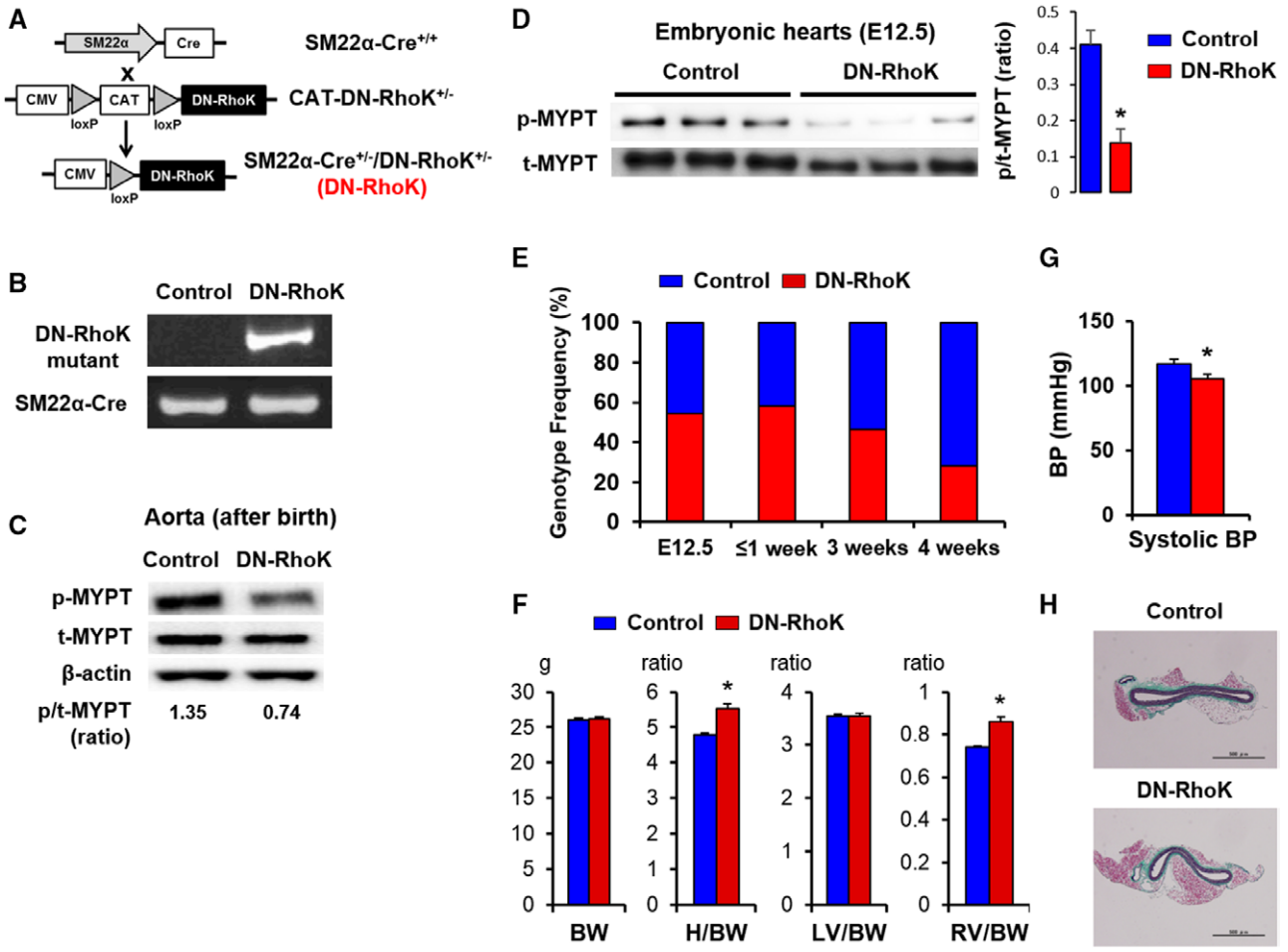

Figure 1. Vascular abnormalities and heart weight changes in dominant-negative Rho-kinase (DN-RhoK) mice. **A**, Homozygous SM22α-Cre transgenic mice (SM22α-Cre$^{+/+}$) were crossed with CAT-DN-RhoK$^{+/-}$ mice, in which the cytomegalovirus (CMV) promoter was separated from the DN-RhoK construct by a chloramphenicol acyltransferase (CAT) gene cassette. In the resulting double-transgenic DN-RhoK mice (SM22α-Cre$^{+/-}$/CAT-DN-RhoK$^{+/-}$), Cre-*loxP* recombination deletes the CAT gene cassette specifically in the cardiovascular system, leading to the expression of the dominant-negative mutant DN-RhoK. **B**, Polymerase chain reaction (PCR) amplification products of genomic DNA from mouse tail biopsies, confirming the presence of the DN-RhoK mutant in DN-RhoK mice and its absence in controls. **C**, Western blot analysis evaluating Rho-kinase activity in the aortas from adult mice. **D**, Western blot analysis evaluating Rho-kinase activity in the hearts from embryonic day 12.5 (E12.5) mice. **E**, Percentages of mice genotyped as DN-RhoK mice at different ages until weaning. E12.5, controls (n=32) and DN-RhoK (n=38); ≤1 week, controls (n=15) and DN-RhoK (n=21); 3 weeks, controls (n=15) and DN-RhoK (n=13); 4 weeks, controls (n=131) and DN-RhoK (n=131). **F**, Mean values of body weight (BW), heart weight (HW)/BW, right ventricular (RV) weight/BW, and left ventricular (LV) weight/BW in 16-week-old mice. n=7 per group. Data are presented as the mean±SEM. *P<0.05 by Student t test. **G**, Systolic blood pressure (BP) was measured using the tail cuff method. n=9–10 per group. Data are presented as the mean±SEM. *P<0.05 by Student t test. **H**, Representative Elastica–Masson staining of the aorta section from a DN-RhoK and a control mouse. Bar, 500 μm. MYPT indicates myosin phosphatase; p-MYPT, phosporylated MYPT; and t-MYPT, total MYPT.

developed sustained ventricular tachycardia and fibrillation and died suddenly during the telemetry ECG follow-up (Figure 3E).

We further examined the effects of Rho-kinase inhibition on cardiovascular performance in DN-RhoK mice. Echocardiographic evaluation of DN-RhoK mice revealed dilated ventricular chambers, especially the RV (Figure 4A). Furthermore, DN-RhoK mice showed increased RV and LV dimensions and reduced LV ejection fraction and fractional shortening compared with controls (Figure 4B), suggesting the involvement of the LV in the cardiac phenotypes of DN-RhoK mice.

Myocardial Fibrofatty Changes in DN-RhoK Mice

We next examined the morphological changes in the heart after birth (Figure 4C). Interestingly, the hearts of DN-RhoK mice were markedly dilated as early as postnatal day 3. The dilatation was more prominent in the RV and was progressive with age (Figure 5A). Cross sections at the level of the ventricles showed a progressive ventricular dilatation and thinning in DN-RhoK hearts, more prominent in the RV, evident from postnatal day 3 (Figure 5A). In contrast, the hearts from controls showed no evidence of ventricular dilatation or thinning (Figure 5B). Myocardial fibrotic changes, though minimal, were evident as early as postnatal day 3 in both the LV and RV in DN-RhoK hearts (Figure 5C). The fibrosis was initially noted in epicardial and perivascular regions of the ventricles in DN-RhoK mice, progressing to the adjacent myocardium with advancing age and involving the entire thickness of the RV free wall in some areas at week 19 (Figure 5C). In contrast, by the age of 19 weeks, control hearts did not show any evidence of

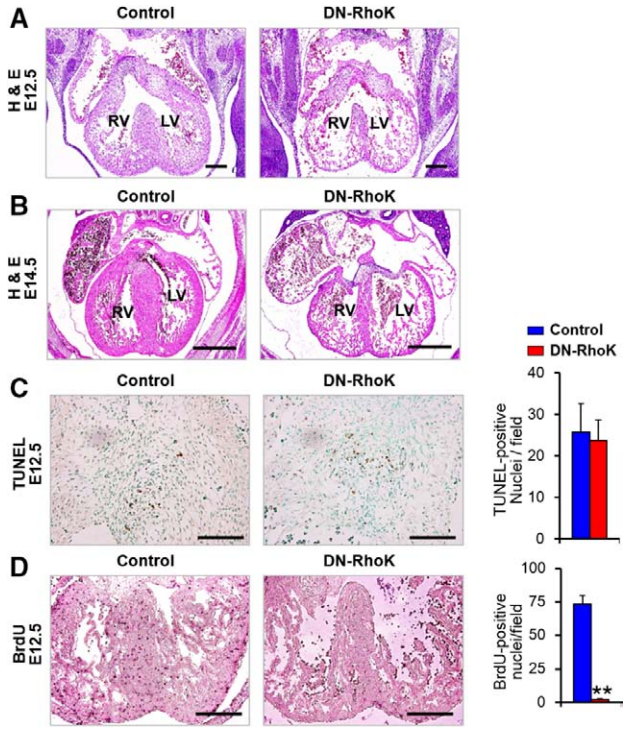

Figure 2. Characteristics of dominant-negative Rho-kinase (DN-RhoK) mice. **A and B**, H&E staining of the embryonic hearts at embryonic day (E12.5; Bar=200 μm; **A**) and E14.5 (Bar=500 μm; **B**). DN-RhoK mice showed marked thinning of the ventricular walls and interventricular septum. **C**, TUNEL (TdT-mediated dUTP nick end labeling) assay showed a comparable number of apoptotic cells (shown as brown nuclei) in the embryonic hearts from E12.5 DN-RhoK and control mice. n=5 for DN-RhoK mice and n=6 for controls. Bar, 100 μm. Data are presented as the mean±SEM. Student *t* test showed no statistically significant differences between the 2 groups. **D**, BrdU (bromodeoxyuridine) assay revealed significantly reduced number of proliferating cardiac cells (shown as purple nuclei) in the hearts from E12.5 DN-RhoK embryos. Data are presented as the mean±SEM. n=3 mice per group. $^{**}P<0.01$ by Student *t* test. Bar, 200 μm. LV indicates left ventricle; and RV, right ventricle.

fibrotic changes in either the RV or the LV (Figure 5D). An additional unexpected observation was the detection of massive fat accumulation in the RV free wall adjacent to the areas of fibrosis in 19-week-old DN-RhoK hearts (Figure 5E), as well as small scattered clusters of fat cells in the LV. No evidence of fatty change was observed in control hearts (Figure 5E). Oil red O staining further confirmed the presence of fatty change mainly in the RV of DN-RhoK mice, and it was not detected in control hearts (Figure 5F, arrows). Our DN-RhoK mice have thereby displayed remarkable and unexpected phenotypes, including cardiac dilatation and dysfunction, myocardial fibrofatty changes, and spontaneous development of ventricular arrhythmias and sudden death. Taken together, these phenotypes fulfill the criteria for ARVC in humans.[20]

Abnormal Myocardial Cell–Cell Junctions in DN-RhoK Mice

ARVC is now widely accepted as a disease of the cardiac desmosome.[2] Interestingly, the Rho/Rho-kinase pathway has been shown to interact with desmosomal proteins possessing intracellular signaling functions.[21,22] Thus, we were interested in examining the ultrastructure of myocardial cell–cell junctions, intercalated discs, where the desmosome resides. Transmission electron microscopy showed widening of the gaps at the intercalated discs in the myocardium of 25-week-old DN-RhoK mice (Figure 5G). In addition, the desmosomes of DN-RhoK mice were less electron-dense compared with the controls (Figure 5G; arrows). The gap width at the desmosomes of DN-RhoK hearts was significantly increased compared with that of control hearts (Figure 5H). These results suggest that normal Rho-kinase function may be necessary for the integrity of cardiac desmosomes.

To further examine the desmosomal abnormalities demonstrated in our mouse model, we next examined the distribution of the desmosomal proteins in ventricular sections by immunofluorescence staining. The expression of plakoglobin was confined to the myocardial cell–cell junctions in the RVs and LVs of control mice (Figure 6). On the contrary, the RVs of DN-RhoK mice displayed a markedly disorganized myocardial structure with poorly defined cell junctional areas. The plakoglobin expression was visibly reduced and, interestingly, was mostly situated at the cardiomyocyte nuclei, rather than at junctional areas (Figure 6). The LV myocardial organization of DN-RhoK heart was more orderly, and though the plakoglobin expression was reduced in intensity compared with control LVs, the signal was mostly present at the myocardial cell–cell junctions (Figure 6). We also stimulated neonatal rat cardiomyocytes with a selective Rho-kinase inhibitor hydroxyfasudil for 24 hours and examined the expression of plakoglobin. However, the expression of plakoglobin did not significantly change by the treatment with hydroxyfasudil (unpublished data). This will be because the impact of Rho-kinase inhibition needs to be chronic during the cardiac development for changing the expression of plakoglobin in heart tissues. Additionally, the expression of Connexin43 was also reduced in DN-RhoK hearts compared with control hearts; the signal was mostly present at the myocardial cell–cell junctions (Figure I in the online-only Data Supplement).

Significantly Altered Gene Expression Profiles in DN-RhoK Hearts

Based on the hypothesis that the Rho-kinase inhibition in DN-RhoK hearts may change the gene profiles responsible for the phenotypes of ARVC, we performed microarray analysis using the Agilent SurePrint G3 Mouse GE microarray kit. The statistical analysis by the statistical computing software R revealed that DN-RhoK hearts had significant changes in 3653 genes (1909 increased and 1744 decreased; $P<0.05$) compared with age-matched controls (E12.5 embryonic hearts). Hierarchical clustering analysis (Figure II in the online-only Data Supplement) and volcano plots analysis (Figure III in the online-only Data Supplement) revealed the significantly altered gene expression profiles in DN-RhoK hearts. Genes with significant changes were further subjected to the pathway analysis using Ingenuity Pathway Analysis software (Ingenuity) to identify gene sets representing specific biological processes or functions. Ingenuity Pathway Analysis software revealed the list of genes significantly

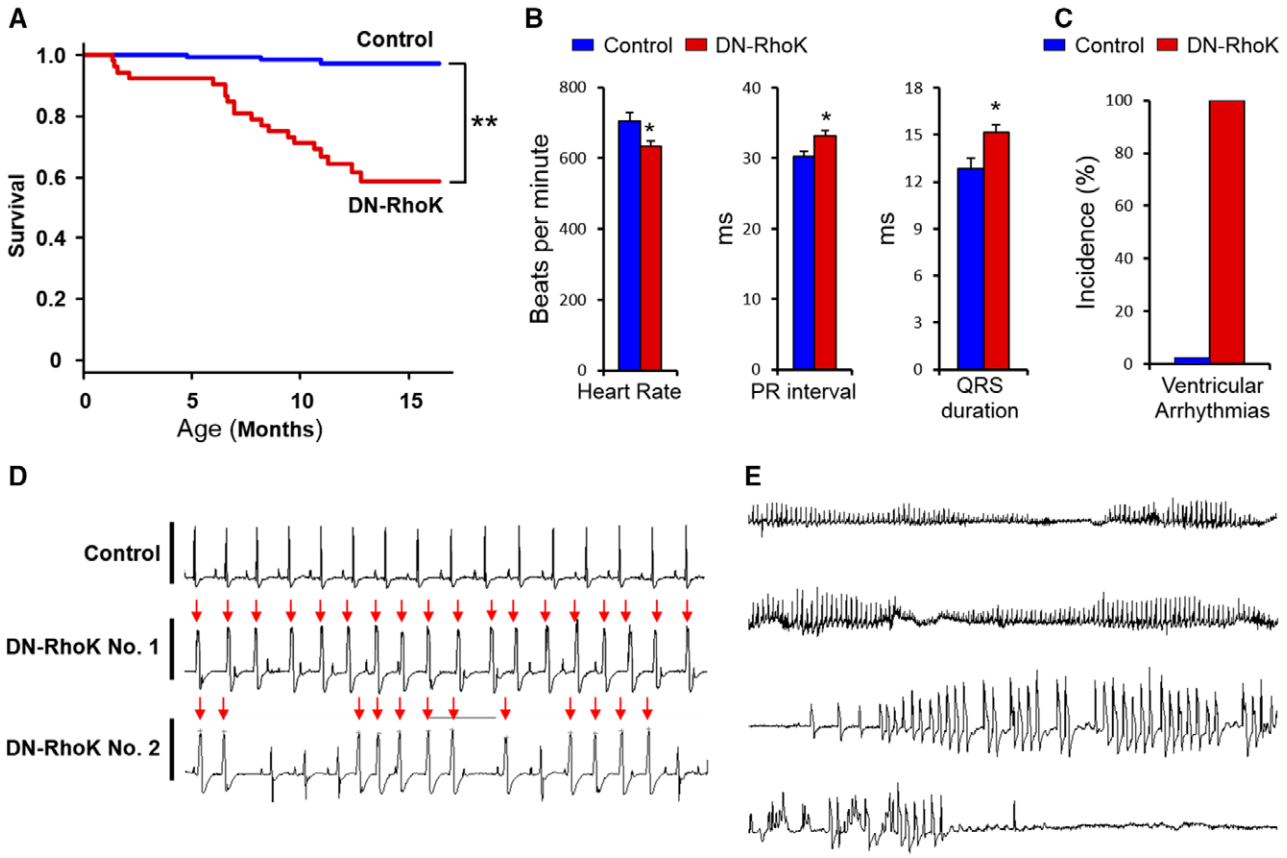

Figure 3. Spontaneous development of ventricular arrhythmias and sudden death in dominant-negative Rho-kinase (DN-RhoK) mice. **A**, Survival curves showing increased mortality rates in DN-RhoK mice (n=52) compared with controls (n=131). ***P*<0.001 by log-rank test. **B**, ECG indices including heart rate, P-R interval, and QRS duration, measured from 10 consecutive beats from single ECG measurements. Data are presented as the mean±SEM. n=4–5 per group. **P*<0.05, ***P*<0.001 by Student *t* test. **C**, Spontaneous ventricular arrhythmias were noted in all DN-RhoK mice, whereas no arrhythmias were noted in control mice. **D**, Representative ECG recordings from one control and 2 different DN-RhoK mice at 14 weeks of age. DN-RhoK mice spontaneously developed frequent ventricular extrasystoles with wide QRS complexes (red arrows). **E**, Sustained ventricular tachycardia, fibrillation, and sudden death in a DN-RhoK mouse during telemetry ECG recording.

upregulated or downregulated in DN-RhoK hearts (Table) and the list of top 25 gene networks (Table I and Figures III–XV in the online-only Data Supplement). Interestingly, among the top up- or downregulated genes, we found many genes associated with the formation of cytoskeleton, cell-to-cell connection, or extracellular matrix (Table), all of which are related with the Rho-kinase signaling. Moreover, several networks were related with the pathways associated with cell morphology, cellular assembly, cell-to-cell interaction, metabolism, connective tissue disorder, and organismal development (Figure IV in the online-only Data Supplement), all of which are consistent with the effects by Rho-kinase inhibition. Consistent with our hypothesis, many genes in the downstream of RhoA signaling were suppressed in the DN-RhoK hearts (Figure V in the online-only Data Supplement). Importantly, cofilin and profilin, both of which are actin-binding proteins and regulate assembly/disassembly of actin filaments, were significantly downregulated in the DN-RhoK hearts. This may cause dysregulation of actin filament, inducing dysfunction of cytoskeletal structure, which may partially explain the histological changes in the hearts of DN-RhoK mice (Figure XVII in the online-only Data Supplement).

Abnormal Wnt Signaling in DN-RhoK Mice

Wnt signaling abnormalities have been recently implicated in the adipogenic phenotype and the pathogenesis of ARVC in mice.[13–15] The Rho-kinase pathway has been shown to regulate adipogenesis through interactions with Wnt signaling.[10,11,23] Thus, we examined the mRNA levels of several genes related to Wnt signaling and adipogenesis. In DN-RhoK mice, the expression levels of peroxisome proliferator activated receptor-γ (PPARγ; *Pparg*), the master regulator of adipogenesis,[24] and Wnt5b (*Wnt5b*), a proadipogenic noncanonical Wnt ligand,[25] were significantly increased in E12.5 hearts compared with control hearts (Figure 7A). In addition, the mRNA level of β-catenin (*Ctnnb1*) and its downstream signaling Axin2 (*Axin2*), the central transcriptional regulator of canonical Wnt/β-catenin signaling,[26] was significantly increased in the E12.5 hearts and in the RV of 3-week-old DN-RhoK mice (Figure 7A; Figure XVIII in the online-only Data Supplement). We further examined the mRNA expression of cardiac stress markers. The expression of connective tissue growth factor (*Ctgf*), one of the earliest growth factors induced in cardiomyocytes in response to hypertrophic stimuli[27] and a powerful profibrotic cytokine,[28] was increased in the 3-week-old RV (Figure 7B). The increased expression

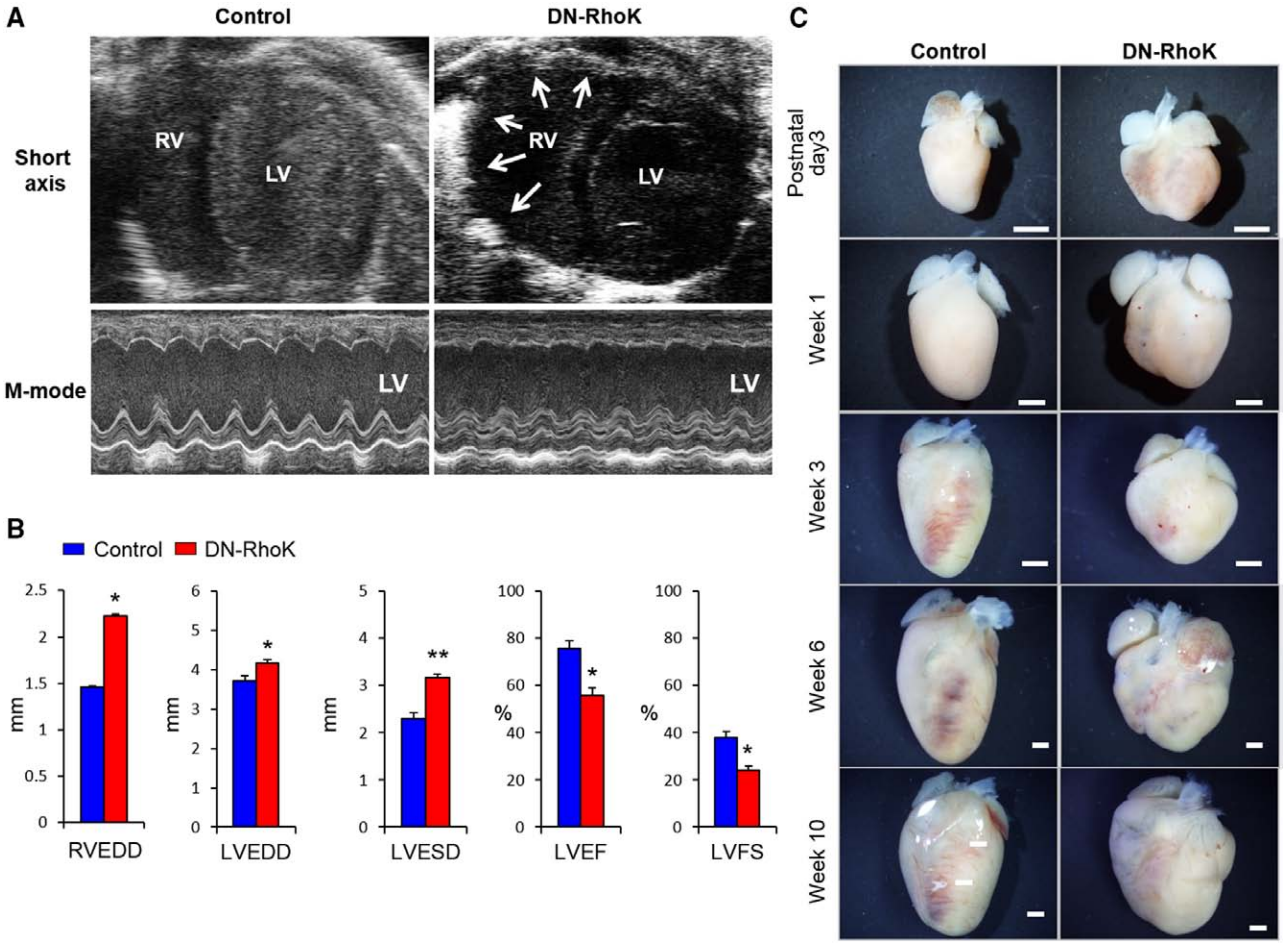

Figure 4. Dominant-negative Rho-kinase (DN-RhoK) mice exhibit cardiac dysfunction and morphological changes. **A**, Transthoracic echocardiography showed biventricular dilatation, to a greater extent in the right ventricle (RV) than in the left ventricle (LV), in DN-RhoK mice. **B**, Echocardiographic parameters in 11-week-old DN-RhoK mice and control mice, including RV end-diastolic diameter (RVEDD), interventricular septum thickness at end systole and end diastole, LV end-systolic and end-diastolic diameters (LVESD and LVEDD, respectively), LV posterior wall systolic and diastolic thickness, LV ejection fraction (LVEF), and LV fractional shortening (LVFS). n=5 per group. Data are presented as the mean±SEM. *P<0.05, **P<0.001 by Student t test. **C**, Gross features of the hearts explanted at postnatal day 3 and weeks 1, 3, 6, and 10, showing progressive enlargement and dilatation, to a greater extent in the RV than in the LV, in DN-RhoK mice. All bars, 1 mm.

of connective tissue growth factor was consistent with the fibrotic changes observed in the hearts of DN-RhoK mice. In addition, the expression of cardiac stress markers, such as atrial natriuretic peptide (*Nppa*) and b-type natriuretic peptide (*Nppb*), were increased in both the embryonic hearts and the 3-week-old RVs (Figure 7B).

Because inhibition of Wnt/β-catenin signaling has been demonstrated in several mouse models of ARVC,[13–15] we further examined the protein levels of Wnt5b, PPARγ, and β-catenin in the DN-RhoK hearts. The protein level of PPARγ in the LV and interventricular septum was comparable between the DN-RhoK hearts and controls (Figure 7C; Figure XVI in the online-only Data Supplement). In contrast, PPARγ levels in the RV were significantly increased in the DN-RhoK hearts compared with controls, pointing toward adipogenic phenotypic change (Figure 7C; Figure XVI in the online-only Data Supplement). Consistently, plakoglobin protein levels were almost half in the DN-RhoK hearts compared with controls (Figure 7D; Figure XVI in the online-only Data Supplement), which is consistent with the immunostaining that revealed a markedly disorganized myocardial structure with poorly defined cell junctional areas (Figure 6). Finally, the downregulation of Rho-kinase activity in DN-RhoK postnatal hearts was mild, probably because of considerable involvement of fibrofatty tissues in DN-RhoK hearts (Figure 7E).

No Myocardial Fibrofatty Change in αMHC-Directed DN-RhoK Mice

To further discriminate the roles of Rho-kinase inhibition before (SM22α-directed) and after (αMHC-directed) the birth, we also developed mice with αMHC (*Myh6*)-directed expression of DN-RhoK. Interestingly, the hearts of 18-week-old αMHC-directed DN-RhoK mice showed no ventricular thinning, RV dilatation, or fibrosis in contrast to the SM22α-directed DN-RhoK mice (Figure XIXA in the online-only Data Supplement). Moreover, these mice developed normally with normal life spans and cardiac structure and function comparable to littermate controls (Figures XIXB and XIXC in the online-only Data Supplement). Because αMHC is mainly a postnatal ventricular gene,[29] intrinsic Rho-kinase activity is

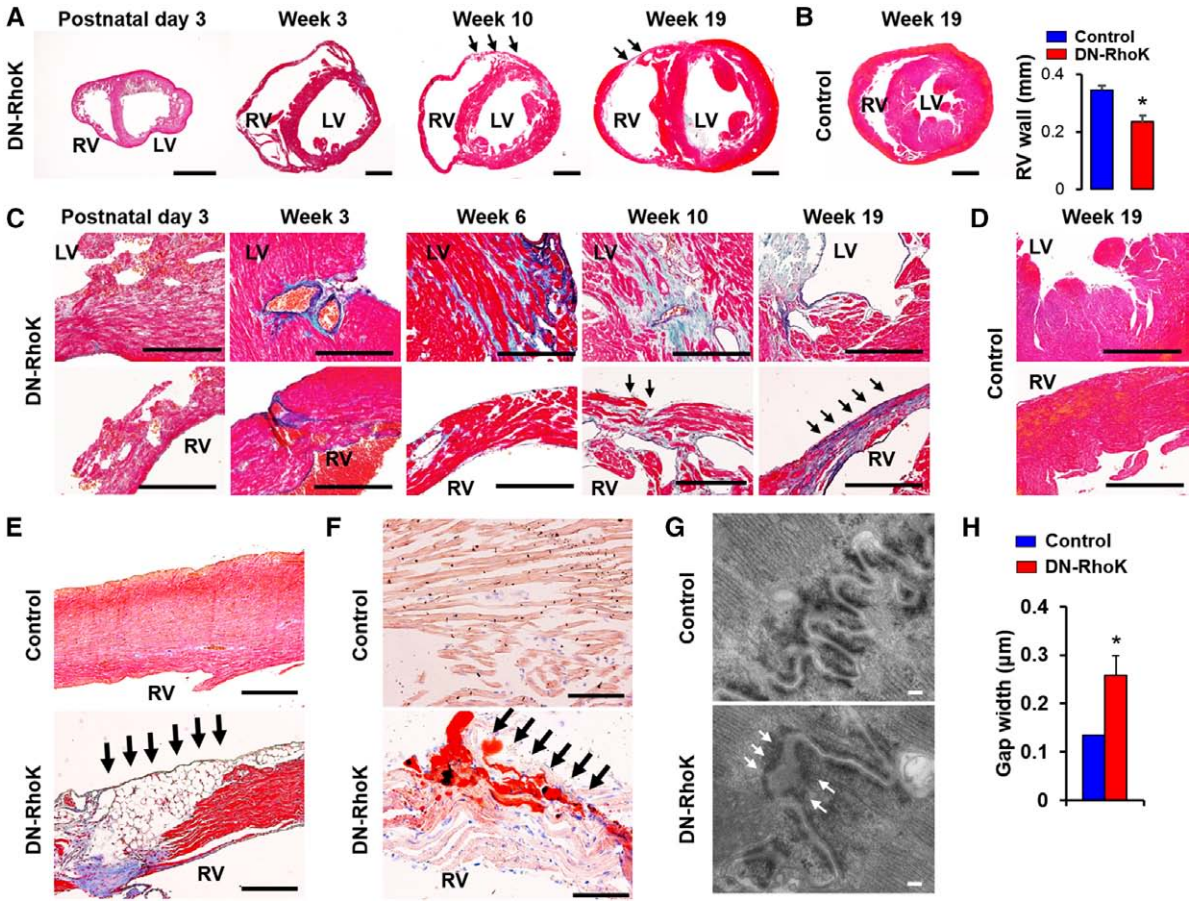

Figure 5. Structural and ultrastructural changes in dominant-negative Rho-kinase (DN-RhoK) hearts. **A–D**, Representative Elastica–Masson staining of the hearts from DN-RhoK mice (postnatal day 3 and weeks 3, 6, 10, and 19) and control mice (week 19). Bar, 1 mm (**A**, **B**) and Bar, 200 μm (**C**, **D**). **E**, Representative Masson-trichrome of the right ventricles (RV) from DN-RhoK mice showing adipogenic deposits next to fibrotic areas at week 19. Bar, 200 μm. **F**, Representative Oil red O staining of the RV confirming the adipogenic changes in DN-RhoK hearts. Bar, 200 μm. **G**, Transmission electron microscopy analysis of the ventricular myocardium showed less electron-dense desmosomes with widened gaps at the intercalated discs (white arrows) in the hearts from DN-RhoK mice at 25 weeks of age. Bar, 100 nm. **H**, Gap width at the myocardial desmosomes in DN-RhoK mice vs controls. Data are presented as the mean±SEM. n=7 intercalated disc areas/mouse. *P<0.05 by Student t test.

most probably inhibited after birth in the hearts of αMHC-directed DN-RhoK mice. In contrast, SM22α is strongly expressed in the developing heart,[30] especially in the RV, thereby inhibiting Rho-kinase activity during embryogenesis in SM22α-directed DN-RhoK mice. Thus, the present findings suggest that Rho-kinase inhibition during early cardiac development promotes abnormal phenotypic changes in the heart, resulting in ARVC.

Discussion

The present study is the first report to implicate Rho-kinase inhibition in the development of ARVC in mice. We have generated a novel mouse model in which Rho-kinase activity is inhibited in the developing heart as early as E7.5.[31] Our DN-RhoK mainly caused cardiac dilatation and dysfunction, myocardial fibrofatty changes, ventricular arrhythmias, and sudden death, fulfilling the criteria for ARVC in humans.[20] Several mouse models of ARVC involving desmosomal gene alterations have been previously developed, including desmoplakin,[13] junction plakoglobin,[14] desmoglein-2,[32] and plakophilin-2.[33] These models have provided additional support to the currently acceptable concept that ARVC is a disease of the desmosome. However, approximately half of the ARVC patients do not harbor any known causative gene mutations,[4] suggesting the involvement of other associated mechanisms. Indeed, the present study suggests that diminished activation of a Rho-kinase signaling pathway could contribute to disease development of ARVC in mice. The recent recognition of the involvement of aberrant Wnt signaling in ARVC pathogenesis in mice[13] support our findings because the Rho/Rho-kinase system are intracellular regulators involved in Wnt signaling pathways.[26] However, there are no previous reports that suggested the involvement of Rho-kinase in the pathophysiology of ARVC in humans. Nevertheless, a recent study aiming at characterizing the ARVC-specific myocardial transcriptome demonstrated the altered regulation of several genes related to Rho-signaling,[34] suggesting that modulation of the Rho/Rho-kinase system may be potentially involved in the pathogenesis of ARVC in humans. The present mouse model provides evidence for the involvement of Rho-kinase inhibition in the pathogenesis of ARVC in mice and may serve as a novel model for ARVC.

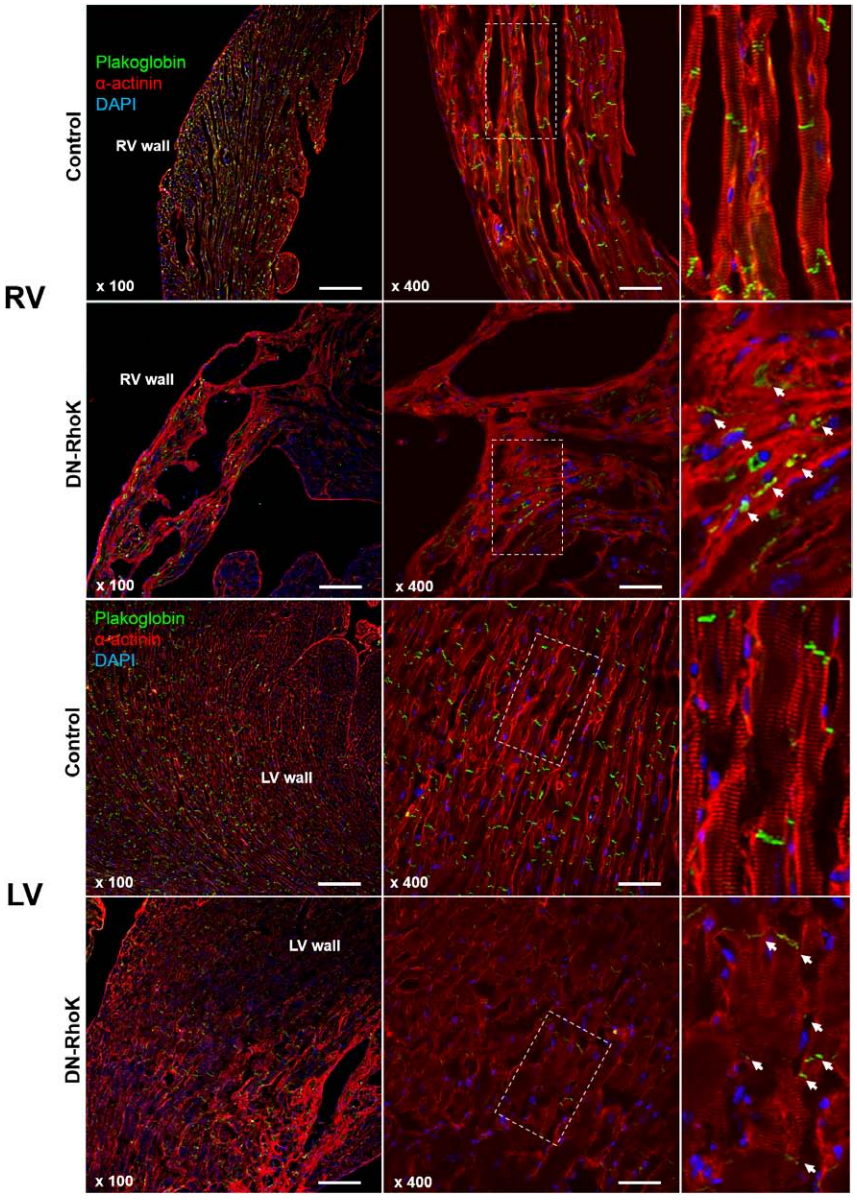

Figure 6. Translocation of plakoglobin to the nucleus in the right ventricles (RV) of dominant-negative Rho-kinase (DN-RhoK) mice. **RV**, Immunofluorescence staining showing the distribution of plakoglobin in the RV of DN-RhoK mice as compared with littermate controls (20 weeks). Note that the plakoglobin signal is situated at the myocardial cell–cell junction in control hearts, whereas the signal is significantly reduced and mostly noted at the nucleus in DN-RhoK hearts. **LV**, Immunofluorescence staining showing the distribution of plakoglobin in the left ventricle (LV) of DN-RhoK mice as compared with littermate controls. Note that the plakoglobin signal is reduced, but is correctly localized to the myocardial cell–cell junction in DN-RhoK hearts, as compared with control hearts. Bar, 200 μm (×100) and 50 μm (×400).

Structural changes in the intercalated discs and desmosomes have been reported in the hearts of ARVC patients,[35] as well as in mouse models of ARVC.[36] These changes most probably result from mechanical disruption of desmosomes secondary to mutated or defective desmosomal proteins. We observed intercalated disc changes in the hearts of our DN-RhoK mice, including less electron-dense desmosomes and widened gaps at the intercalated discs, in which Rho-kinase will organize cytoskeletal filaments and supports desmosomal protein complex. Consistent with our findings, the Rho/Rho-kinase pathway has been shown to be necessary for normal desmosomal assembly.[21] In addition, recent studies have demonstrated a cross talk between the Rho/Rho-kinase pathway, on the one hand, and the intracellular signaling pathways involving the desmosomal proteins of the armadillo family, including plakophilin-2[22] and plakoglobin, on the other hand.[22] Interestingly, plakoglobin was reduced at the myocardial cell–cell junctions and the intercalated discs and was translocated to the nucleus in the RV of DN-RhoK mice. Loss of plakoglobin at the intercalated discs and reduction of protein levels may offer an explanation for the structural changes observed by electron microscopy. The nuclear relocalization of plakoglobin was similar to that observed in the mouse models developed by Garcia-Gras et al[13] and Lombardi et al,[14] where plakoglobin inhibits Wnt/β-catenin signaling through competing with β-catenin for its transcriptional targets, thereby stimulating adipogenic programming of the cardiomyocyte. In those studies, the trigger for the nuclear translocation of plakoglobin was the presence of desmosomal protein mutation.[13] In the absence of desmosomal mutation in our mouse model, the nuclear translocation of plakoglobin might be explained by the recently uncovered role for RhoA signaling in the assembly of desmosome protein complex (Figure 8). Godsel et al[21] have demonstrated that the RhoA-mediated actin reorganization is necessary for directing desmosomal precursors enriched in desmoplakin to sites of cell–cell contacts to be

Table. List of the Genes Upregulated or Downregulated in DN-RhoK Compared With Control Embryonic Hearts (E12.5)

Symbol	Gene Name	DN-RhoK/WT (E12.5 heart, fold)	*P* Value	Q Value
Upregulated genes in DN-RhoK mice				
C14orf159	Chromosome 14 open reading frame 159	2.821	0.020	0.2152
ADAMTS2	ADAM metallopeptidase with thrombospondin type 1 motif, 2	2.721	0.047	0.2596
GDF15	Growth differentiation factor 15	2.469	0.034	0.2389
TRIB3	Tribbles homolog 3 (Drosophila)	2.180	0.010	0.1959
ANXA8L2	Annexin A8-like 2	2.004	0.022	0.2213
GRIA3	Glutamate receptor, ionotropic, AMPA 3	2.000	0.018	0.2113
LRRC17	Leucine-rich repeat containing 17	1.979	0.049	0.2629
LUM	Lumican	1.951	0.048	0.2612
FAS	Fas cell surface death receptor	1.951	0.024	0.2238
ANXA1	Annexin A1	1.936	0.017	0.2107
Downregulated genes in DN-RhoK mice				
SYT10	Synaptotagmin X	0.066	0.002	0.1764
SOX1	SRY (sex determining region Y)-box 1	0.340	0.001	0.1764
ITGA5	Integrin, α5 (fibronectin receptor, α polypeptide)	0.411	0.003	0.1764
ACTN1	Actinin, α1	0.443	0.007	0.1877
INPP5E	Inositol polyphosphate-5-phosphatase	0.448	0.032	0.2360
ZFP57	ZFP57 zinc finger protein	0.480	0.014	0.2058
CNOT3	CCR4-NOT transcription complex, subunit 3	0.483	0.011	0.1959
MARK2	MAP/microtubule affinity-regulating kinase 2	0.484	0.005	0.1843
DTX3	Deltex homolog 3 (Drosophila)	0.485	0.006	0.1859
HSPG2	Heparan sulfate proteoglycan 2	0.488	<0.001	0.1764

The number of samples is 4 in each group.

incorporated into newly forming desmosomes. In that study, pharmacological inhibition of Rho-kinase inhibited desmoplakin border accumulation. In our DN-RhoK model, microarray analysis demonstrated significant alterations in genes responsible for actin fiber assembly and cytoskeletal reorganization. Thus, considering the early embryonic Rho-kinase inhibition in our mouse model, the direction of desmoplakin-enriched desmosomal precursors to the cell border and the subsequent incorporation into newly formed desmosomes might have been impaired. Plakoglobin, which anchors desmoplakin to the intermediate filament network, will consequently fail to incorporate into the desmosome and is available to translocate to the nucleus (Figure 8). Nuclear plakoglobin competes with β-catenin for its transcriptional factors, thereby inhibiting Wnt/β-catenin signaling.[13] The increased protein levels of β-catenin and Axin2 in the RV of DN-RhoK mice may reflect the positive feedback.

Adipogenic replacement of the myocardium is an important pathological feature of ARVC.[37] The hearts of DN-RhoK mice exhibited marked myocardial fatty change, which is interesting because fat tissue is normally rare in the mouse heart.[38] In addition, the adipogenic phenotype has been displayed only in a few desmosomal mouse models of ARVC, with aberrations of Wnt signaling found to be involved.[13] These studies have shown that, in response to desmosomal protein mutation, the desmosomal protein plakoglobin is translocated to the nucleus, where it inhibits Wnt/β-catenin signaling through competing with β-catenin for its transcriptional targets.[14] Inhibition of Wnt/β-catenin signaling will promote adipogenesis and is believed to be responsible for a developmental myogenic–adipogenic switch in cardiac progenitor cells.[13] Those studies have also demonstrated increased expression levels of the proadipogenic noncanonical Wnt ligand, Wnt5b, and have suggested Wnt5b as a potential mediator in ARVC pathogenesis.[14] As mentioned earlier, there is an established role for the Rho/Rho-kinase pathway in the regulation of adipogenesis. Inhibition of the Rho-kinase system in vitro, both pharmacologically and genetically, has been shown to promote adipogenesis.[39] In addition, the Rho-kinase system plays an important role in regulating the adipogenesis–myogenesis cell fate decision.[40] Several studies have shown that Rho-kinase regulates adipogenesis through interaction with Wnt signaling[11,23] and, in part, by regulating the expression of pro- and antiadipogenic Wnt genes, where Rho-kinase inhibition stimulates the expression of proadipogenic Wnt genes, whereas Rho-kinase activation stimulates the expression of antiadipogenic Wnt genes.[10] In addition, recent studies have suggested that Rho-kinase is also involved in adipogenesis through regulating the expression of

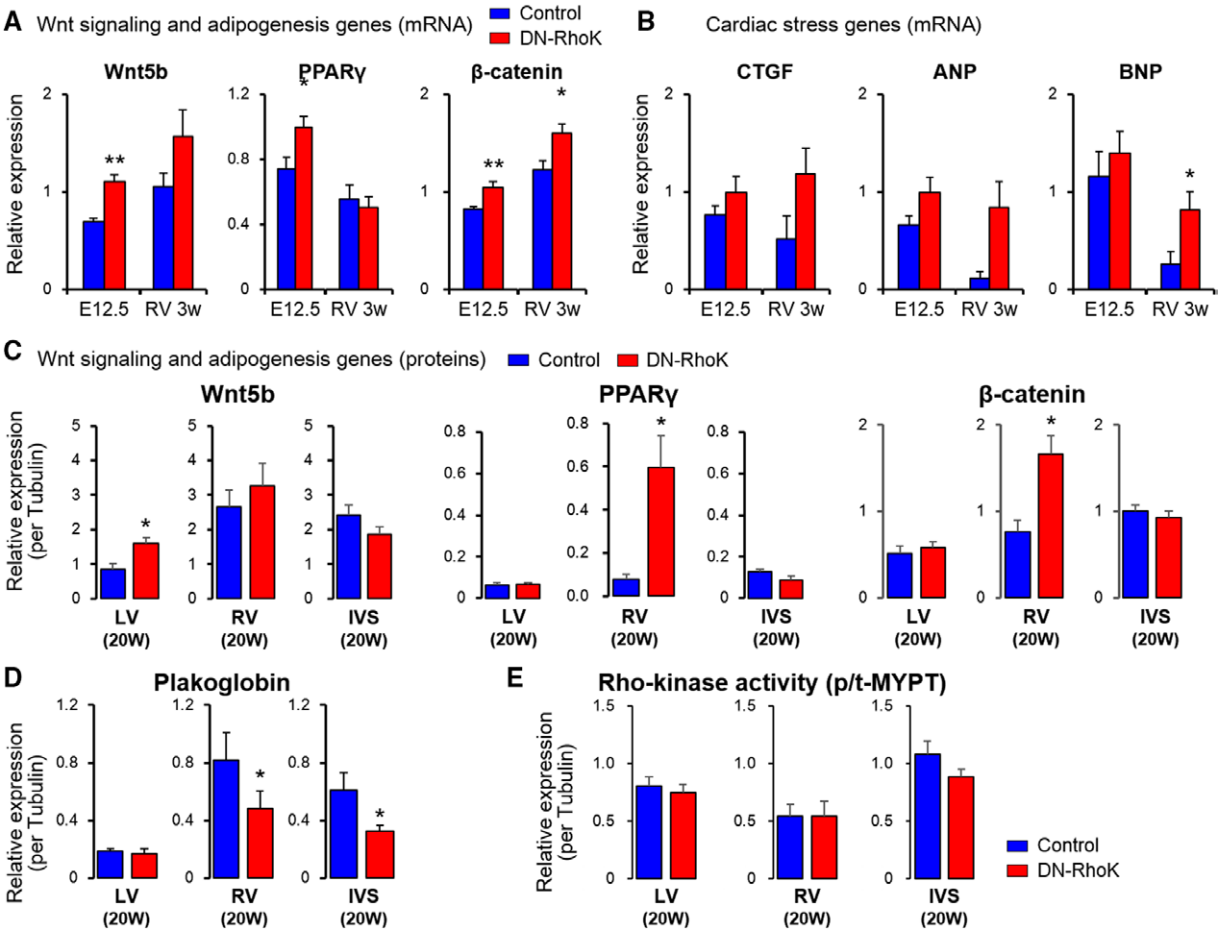

Figure 7. Molecular alterations in the dominant-negative Rho-kinase (DN-RhoK) heart. **A** and **B**, Relative gene expression of Wnt signaling and adipogenesis genes (**A**, Wnt5b, peroxisome proliferator activated receptor-γ [PPARγ], and β-catenin) and cardiac stress genes (**B**, CTGF, ANP, and BNP) in embryonic day (E) 12.5 hearts and the right ventricle (RV) of 3-week-old (w) mice. Relative expression levels are normalized to *Gapdh*. E12.5 hearts, n=4 for control and n=6 for DN-RhoK mice. RV 3w, n=6 for control and n=8 for DN-RhoK mice. Data are presented as the mean±SEM. **P*<0.05, ***P*<0.001 by Student *t* test. **C**, Western blots of Wnt signaling and adipogenesis genes (Wnt5b, PPARγ, and β-catenin) of the adult hearts (20 weeks old) showing increased expression of Wnt5b, PPARγ, and β-catenin especially in the RV of DN-RhoK hearts. n=5 per group. **D**, Western blots of adult hearts (20 weeks old) showing reduced expression of plakoglobin, especially in the RV and interventricular septum (IVS) of DN-RhoK hearts. n=5 per group. **P*<0.05 by Student *t* test. **E**, Western blots of adult hearts (20 weeks old) showing slightly reduced activities in DN-RhoK hearts. n=5 per group. **P*<0.05 by Student *t* test. ANP indicates atrial natriuretic peptide; BNP, b-type natriuretic peptide; and CTGF, connective tissue growth factor.

PPARγ, the master regulator of adipogenesis,[24] and β-catenin, the central transcriptional regulator of canonical Wnt/β-catenin signaling,[26] where Rho-kinase inhibition promotes adipogenesis through upregulating PPARγ and downregulating β-catenin.[23] In the present study, we have demonstrated that Rho-kinase inhibition was associated with a significant increase in the expression levels of Wnt5b, PPARγ, and β-catenin in the hearts of DN-RhoK mice (Figure 7C). Wnt5b has been shown to stimulate adipogenesis by directly increasing the expression levels of PPARγ[41] and through inhibition of Wnt/β-catenin signaling by preventing nuclear translocation of β-catenin. Microarray data also highlight a role for Tax1bp3 (Figure VI in the online-only Data Supplement), which binds to β-catenin and inhibits its transcriptional activity.[42] Thus, the present results suggest that Rho-kinase inhibition mediates the inhibition of Wnt/β-catenin signaling, and cytoskeletal filament disorganization may be responsible for the impaired desmosomal protein complex and possibly the pathogenesis of ARVC in our mouse model (Figure 8).

The disease process started prenatally in our mouse model, as reflected by the cardiac structural changes. Prenatal onset has been reported in some desmosomal mouse models of ARVC.[13] In human ARVC, the diagnosis might be difficult before the age of 10 years,[1] although cases of ARVC in infants,[43] and even in the embryo,[44] have also been reported. In the present study, we have demonstrated that Rho-kinase deficiency in the embryonic heart resulted in abnormal cardiac development, involving ventricular thinning and reduced cardiac proliferation. These findings are consistent with the results of the previous studies that have used pharmacological inhibition of Rho-kinase in cultured mouse embryos, starting from E7.5 to E8.0.[45,46] Those studies implicated Rho-kinase in the regulation of cardiac cell proliferation through controlling the expression of cell cycle proteins.[45,46] It has been shown that Rho-kinase inhibition downregulates the expression of β-catenin and its downstream target cyclin-D1,[23] suggesting that the reduced cardiac cell proliferation mediated by Rho-kinase inhibition may be partially caused by reduced

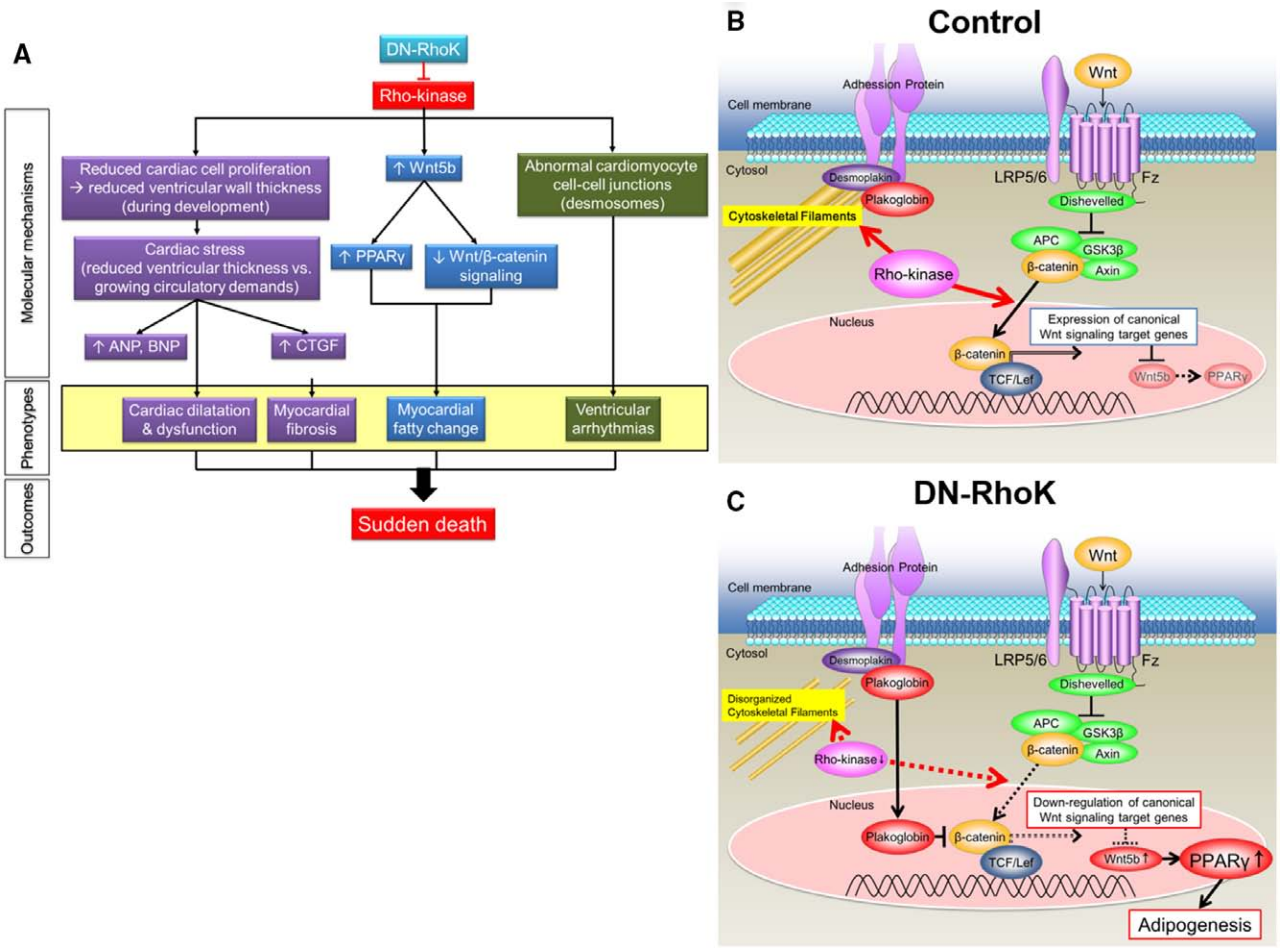

Figure 8. Rho-kinase signaling organizes cytoskeletal filaments and desmosomal structure. The transcriptional effects of Wnt are mediated by the nuclear translocation of β-catenin and the subsequent recruitment of TCF/Lef DNA-binding factors as coactivators for transcription. Plakoglobin is a cytoplasmic protein that consists of the submembranous plaques of desmosomes. In the dominant-negative Rho-kinase (DN-RhoK) embryonic heart, the desmosomal protein plakoglobin is translocated to the nucleus, where it inhibits Wnt/β-catenin signaling through competing with β-catenin for its transcriptional targets of TCF/Lef DNA-binding factors. **B and C**, The role of Rho-kinase inhibition in the development of arrhythmogenic right ventricular cardiomyopathy (ARVC) in DN-RhoK mice. Rho-kinase inhibition in the developing heart results in the development of ARVC phenotypes in DN-RhoK mice through 3 mechanisms: (1) reduction of cardiac cell proliferation and ventricular wall thickness, (2) stimulation of the expression of the proadipogenic noncanonical Wnt ligand, Wnt5b, and the major adipogenic transcription factor, peroxisome proliferator activated receptor-γ (PPARγ), and inhibition of Wnt/β-catenin signaling, and (3) development of desmosomal abnormalities. These mechanisms lead to the development of cardiac dilatation and dysfunction, myocardial fibrofatty changes, and ventricular arrhythmias, ultimately resulting in sudden premature death in this ARVC mouse model. ANP indicates atrial natriuretic peptide; BNP, b-type natriuretic peptide; and CTGF, connective tissue growth factor.

Wnt/β-catenin signaling. Our microarray data also stress the involvement of Rho-kinase functional networks related to pathways associated with cell morphology, cellular assembly, and organismal development. Among the top downregulated genes, α-actinin has been shown to colocalize with the proteins in the adherens junctions at the intercalated disc,[47] where it acts as the linkage with the actin filament. Thus, reduction of α-actinin may have induced the detachment of actin filaments at the intercalated disc and dysfunction of cell-to-cell attachment of cardiac myocytes. The Ingenuity Pathway Analysis network with the highest score showed the downregulation of transforming growth factor-β, an important growth factor for the development of various organs (Figure VI in the online-only Data Supplement). Transforming growth factor-β plays a crucial role in the development of cardiac dysfunction and fibrosis after pressure overload in mice.[48] Transforming growth factor-β3 (encoded by *TGFB3*) is known as one of the causative genes for the development of familial ARVC.[49] These reports and our present findings suggest that the downregulation of transforming growth factor-β may have promoted the development of fibrofatty changes and the phenotypes of ARVC in DN-RhoK hearts.

Finally, we have performed experiments to examine the role of Rho-kinase in the regulation of calcium currents in myocytes of the RV. Here, it was difficult to obtain intact isolated myocytes from DN-RhoK hearts because of its fibrofatty changes and fragile structure of the RV. Thus, we used trabeculae from the RV of rats to confirm the role of Rho-kinase inhibition in the RV. Interestingly, Rho-kinase inhibition by selective Rho-kinase inhibitor, hydroxyfasudil, did not significantly reduce force nor $[Ca]_i$ in the RV trabeculae of rats ex vivo (unpublished data).

To summarize the role of Rho-kinase inhibition in our DN-RhoK mice, we have shown that Rho-kinase inhibition in the developing heart results in the development of ARVC through the following 3 mechanisms (Figure 8). First, Rho-kinase inhibition in the developing heart reduces cardiac cell proliferation and ventricular wall thickness. We consider that the attenuated myocardium fails to withstand the growing circulatory demands of the developing cardiovascular system, eventually resulting in cardiac dilatation and dysfunction. The cardiac stress is reflected by the increased expression of the profibrotic cytokine, connective tissue growth factor, resulting in a progressive myocardial fibrosis. Second, Rho-kinase inhibition possibly stimulates the expression of Wnt5b and PPARγ, which may be responsible for the myocardial fatty change in our mouse model. Third, inhibition of Rho-kinase is responsible for the abnormalities of the intercalated discs and desmosomes detected. The myocardial fibrofatty changes and the aberrant cell–cell communication may explain the ventricular arrhythmias that ultimately resulted in the sudden premature death in this ARVC model. Thus, Rho-kinase inhibition may offer an explanation for the development of the seemingly unrelated cardiac changes observed in ARVC and may justify Rho-kinase as a novel target to be explored in ARVC. Interactions between the Rho-kinase pathway and the Wnt signaling pathway would offer a plausible new insight into the pathogenesis of the important but yet incompletely understood disorder, ARVC.

Our present findings support a crucial role for Rho-kinase in cardiac development and may warn against the use of Rho-kinase inhibitors during pregnancy. Rho-kinase plays a crucial role in the development of cardiovascular diseases.[6,7] The beneficial effects of Rho-kinase inhibition for the treatment of cardiovascular disease have been demonstrated in various animal models and in humans.[6] However, based on the present study, Rho-kinase inhibitor may adversely affect the fetus, which is similar to the inhibitors of renin–angiotensin system. The renin–angiotensin system plays a crucial role during the normal pregnancy and subsequent well-being of mother and fetus.[50] Therefore, the use of renin–angiotensin system inhibitors is contraindicated in pregnant women.[50] To date, we have demonstrated that several medications, including statins, calcium channel blockers, and eicosapentaenoic acid, have an indirect inhibitory effect for Rho-kinase.[6,7] Thus, the high dosage of these drugs during pregnancy may potentially contribute to the development of ARVC, which should be considered as a potential mechanism in the cases of unknown origin.

Acknowledgments

Alia Ellawindy is a recipient of a scholarship from the Honjo International Scholarship Foundation and received the first place of the 2013 Young Investigator Award for International Students by the Japanese Circulation Society for the present study. We are grateful to the laboratory members in the Department of Cardiovascular Medicine at Tohoku University for valuable technical assistance, especially Hiromi Yamashita, Ai Nishihara, and Yumi Watanabe.

Sources of Funding

This work was supported in part by the Takeda Science Foundation, the grant-in-aid for Tohoku University Global COE for Conquest of Signal Transduction Diseases with Network Medicine, and the grants-in-aid for Scientific Research (21790698, 23659408, 24390193, 15H02535, 15H04816, and 15K15046), all of which are from the Ministry of Education, Culture, Sports, Science and Technology, Tokyo, Japan; and the grants-in-aid for Scientific Research from the Ministry of Health, Labor, and Welfare, Tokyo, Japan (10102895, 15545346).

Disclosures

None.

References

1. Basso C, Corrado D, Marcus FI, Nava A, Thiene G. Arrhythmogenic right ventricular cardiomyopathy. *Lancet*. 2009;373:1289–1300. doi: 10.1016/S0140-6736(09)60256-7.
2. Delmar M, McKenna WJ. The cardiac desmosome and arrhythmogenic cardiomyopathies: from gene to disease. *Circ Res*. 2010;107:700–714. doi: 10.1161/CIRCRESAHA.110.223412.
3. Awad MM, Calkins H, Judge DP. Mechanisms of disease: molecular genetics of arrhythmogenic right ventricular dysplasia/cardiomyopathy. *Nat Clin Pract Cardiovasc Med*. 2008;5:258–267. doi: 10.1038/ncpcardio1182.
4. Corrado D, Basso C, Pilichou K, Thiene G. Molecular biology and clinical management of arrhythmogenic right ventricular cardiomyopathy/dysplasia. *Heart*. 2011;97:530–539. doi: 10.1136/hrt.2010.193276.
5. Marcus F, Towbin JA. The mystery of arrhythmogenic right ventricular dysplasia/cardiomyopathy: from observation to mechanistic explanation. *Circulation*. 2006;114:1794–1795. doi: 10.1161/CIRCULATIONAHA.106.653493.
6. Shimokawa H, Takeshita A. Rho-kinase is an important therapeutic target in cardiovascular medicine. *Arterioscler Thromb Vasc Biol*. 2005;25:1767–1775. doi: 10.1161/01.ATV.0000176193.83629.c8.
7. Satoh K, Fukumoto Y, Shimokawa H. Rho-kinase: important new therapeutic target in cardiovascular diseases. *Am J Physiol Heart Circ Physiol*. 2011;301:H287–H296. doi: 10.1152/ajpheart.00327.2011.
8. Amano M, Fukata Y, Kaibuchi K. Regulation and functions of Rho-associated kinase. *Exp Cell Res*. 2000;261:44–51. doi: 10.1006/excr.2000.5046.
9. Riento K, Ridley AJ. Rocks: multifunctional kinases in cell behaviour. *Nat Rev Mol Cell Biol*. 2003;4:446–456. doi: 10.1038/nrm1128.
10. Cristancho AG, Lazar MA. Forming functional fat: a growing understanding of adipocyte differentiation. *Nat Rev Mol Cell Biol*. 2011;12:722–734. doi: 10.1038/nrm3198.
11. Schlessinger K, Hall A, Tolwinski N. Wnt signaling pathways meet Rho GTPases. *Genes Dev*. 2009;23:265–277. doi: 10.1101/gad.1760809.
12. Angers S, Moon RT. Proximal events in Wnt signal transduction. *Nat Rev Mol Cell Biol*. 2009;10:468–477. doi: 10.1038/nrm2717.
13. Garcia-Gras E, Lombardi R, Giocondo MJ, Willerson JT, Schneider MD, Khoury DS, Marian AJ. Suppression of canonical Wnt/beta-catenin signaling by nuclear plakoglobin recapitulates phenotype of arrhythmogenic right ventricular cardiomyopathy. *J Clin Invest*. 2006;116:2012–2021. doi: 10.1172/JCI27751.
14. Lombardi R, Dong J, Rodriguez G, Bell A, Leung TK, Schwartz RJ, Willerson JT, Brugada R, Marian AJ. Genetic fate mapping identifies second heart field progenitor cells as a source of adipocytes in arrhythmogenic right ventricular cardiomyopathy. *Circ Res*. 2009;104:1076–1084. doi: 10.1161/CIRCRESAHA.109.196899.
15. Lombardi R, da Graca Cabreira-Hansen M, Bell A, Fromm RR, Willerson JT, Marian AJ. Nuclear plakoglobin is essential for differentiation of cardiac progenitor cells to adipocytes in arrhythmogenic right ventricular cardiomyopathy. *Circ Res*. 2011;109:1342–1353. doi: 10.1161/CIRCRESAHA.111.255075.
16. Amano M, Chihara K, Nakamura N, Fukata Y, Yano T, Shibata M, Ikebe M, Kaibuchi K. Myosin II activation promotes neurite retraction during the action of Rho and Rho-kinase. *Genes Cells*. 1998;3:177–188.
17. Amano M, Chihara K, Nakamura N, Kaneko T, Matsuura Y, Kaibuchi K. The COOH terminus of Rho-kinase negatively regulates rho-kinase activity. *J Biol Chem*. 1999;274:32418–32424.
18. Kobayashi K, Takahashi M, Matsushita N, Miyazaki J, Koike M, Yaginuma H, Osumi N, Kaibuchi K, Kobayashi K. Survival of developing motor neurons mediated by Rho GTPase signaling pathway through Rho-kinase. *J Neurosci*. 2004;24:3480–3488. doi: 10.1523/JNEUROSCI.0295-04.2004.

19. Kaufman MH. *The Atlas of Mouse Development*. Amsterdam, Heidelberg [u.a.]: Elsevier Academic Press; 2010.
20. Marcus FI, McKenna WJ, Sherrill D, et al. Diagnosis of arrhythmogenic right ventricular cardiomyopathy/dysplasia: proposed modification of the task force criteria. *Circulation*. 2010;121:1533–1541. doi: 10.1161/CIRCULATIONAHA.108.840827.
21. Godsel LM, Dubash AD, Bass-Zubek AE, Amargo EV, Klessner JL, Hobbs RP, Chen X, Green KJ. Plakophilin 2 couples actomyosin remodeling to desmosomal plaque assembly via RhoA. *Mol Biol Cell*. 2010;21:2844–2859. doi: 10.1091/mbc.E10-02-0131.
22. Todorović V, Desai BV, Patterson MJ, Amargo EV, Dubash AD, Yin T, Jones JC, Green KJ. Plakoglobin regulates cell motility through Rho- and fibronectin-dependent Src signaling. *J Cell Sci*. 2010;123(pt 20):3576–3586. doi: 10.1242/jcs.070391.
23. Li L, Tam L, Liu L, Jin T, Ng DS. Wnt-signaling mediates the anti-adipogenic action of lysophosphatidic acid through cross talking with the Rho/Rho associated kinase (ROCK) pathway. *Biochem Cell Biol*. 2011;89:515–521. doi: 10.1139/o11-048.
24. Christodoulides C, Lagathu C, Sethi JK, Vidal-Puig A. Adipogenesis and WNT signalling. *Trends Endocrinol Metab*. 2009;20:16–24. doi: 10.1016/j.tem.2008.09.002.
25. Kanazawa A, Tsukada S, Kamiyama M, Yanagimoto T, Nakajima M, Maeda S. Wnt5b partially inhibits canonical Wnt/beta-catenin signaling pathway and promotes adipogenesis in 3T3-L1 preadipocytes. *Biochem Biophys Res Commun*. 2005;330:505–510. doi: 10.1016/j.bbrc.2005.03.007.
26. Rao TP, Kühl M. An updated overview on Wnt signaling pathways: a prelude for more. *Circ Res*. 2010;106:1798–1806. doi: 10.1161/CIRCRESAHA.110.219840.
27. Kemp TJ, Aggeli IK, Sugden PH, Clerk A. Phenylephrine and endothelin-1 upregulate connective tissue growth factor in neonatal rat cardiac myocytes. *J Mol Cell Cardiol*. 2004;37:603–606. doi: 10.1016/j.yjmcc.2004.04.022.
28. Chen MM, Lam A, Abraham JA, Schreiner GF, Joly AH. CTGF expression is induced by TGF- beta in cardiac fibroblasts and cardiac myocytes: a potential role in heart fibrosis. *J Mol Cell Cardiol*. 2000;32:1805–1819. doi: 10.1006/jmcc.2000.1215.
29. Ng WA, Grupp IL, Subramaniam A, Robbins J. Cardiac myosin heavy chain mRNA expression and myocardial function in the mouse heart. *Circ Res*. 1991;68:1742–1750.
30. Li L, Miano JM, Cserjesi P, Olson EN. SM22 alpha, a marker of adult smooth muscle, is expressed in multiple myogenic lineages during embryogenesis. *Circ Res*. 1996;78:188–195.
31. Yang M, Jiang H, Li L. Sm22α transcription occurs at the early onset of the cardiovascular system and the intron 1 is dispensable for its transcription in smooth muscle cells during mouse development. *Int J Physiol Pathophysiol Pharmacol*. 2010;2:12–19.
32. Pilichou K, Remme CA, Basso C, et al. Myocyte necrosis underlies progressive myocardial dystrophy in mouse dsg2-related arrhythmogenic right ventricular cardiomyopathy. *J Exp Med*. 2009;206:1787–1802. doi: 10.1084/jem.20090641.
33. Cerrone M, Noorman M, Lin X, Chkourko H, Liang FX, van der Nagel R, Hund T, Birchmeier W, Mohler P, van Veen TA, van Rijen HV, Delmar M. Sodium current deficit and arrhythmogenesis in a murine model of plakophilin-2 haploinsufficiency. *Cardiovasc Res*. 2012;95:460–468. doi: 10.1093/cvr/cvs218.
34. Gaertner A, Schwientek P, Ellinghaus P, Summer H, Golz S, Kassner A, Schulz U, Gummert J, Milting H. Myocardial transcriptome analysis of human arrhythmogenic right ventricular cardiomyopathy. *Physiol Genomics*. 2012;44:99–109. doi: 10.1152/physiolgenomics.00094.2011.
35. Basso C, Czarnowska E, Della Barbera M, et al. Ultrastructural evidence of intercalated disc remodelling in arrhythmogenic right ventricular cardiomyopathy: an electron microscopy investigation on endomyocardial biopsies. *Eur Heart J*. 2006;27:1847–1854. doi: 10.1093/eurheartj/ehl095.
36. Yang Z, Bowles NE, Scherer SE, et al. Desmosomal dysfunction due to mutations in desmoplakin causes arrhythmogenic right ventricular dysplasia/cardiomyopathy. *Circ Res*. 2006;99:646–655. doi: 10.1161/01.RES.0000241482.19382.c6.
37. Basso C, Bauce B, Corrado D, Thiene G. Pathophysiology of arrhythmogenic cardiomyopathy. *Nat Rev Cardiol*. 2012;9:223–233. doi: 10.1038/nrcardio.2011.173.
38. Lodder EM, Rizzo S. Mouse models in arrhythmogenic right ventricular cardiomyopathy. *Front Physiol*. 2012;3:221. doi: 10.3389/fphys.2012.00221.
39. Noguchi M, Hosoda K, Fujikura J, Fujimoto M, Iwakura H, Tomita T, Ishii T, Arai N, Hirata M, Ebihara K, Masuzaki H, Itoh H, Narumiya S, Nakao K. Genetic and pharmacological inhibition of Rho-associated kinase II enhances adipogenesis. *J Biol Chem*. 2007;282:29574–29583. doi: 10.1074/jbc.M705972200.
40. Sordella R, Jiang W, Chen GC, Curto M, Settleman J. Modulation of Rho GTPase signaling regulates a switch between adipogenesis and myogenesis. *Cell*. 2003;113:147–158.
41. van Tienen FH, Laeremans H, van der Kallen CJ, Smeets HJ. Wnt5b stimulates adipogenesis by activating PPARgamma, and inhibiting the beta-catenin-dependent Wnt signaling pathway together with Wnt5a. *Biochem Biophys Res Commun*. 2009;387:207–211. doi: 10.1016/j.bbrc.2009.07.004.
42. Kanamori M, Sandy P, Marzinotto S, Benetti R, Kai C, Hayashizaki Y, Schneider C, Suzuki H. The PDZ protein tax-interacting protein-1 inhibits beta-catenin transcriptional activity and growth of colorectal cancer cells. *J Biol Chem*. 2003;278:38758–38764. doi: 10.1074/jbc.M306324200.
43. Turrini P, Basso C, Daliento L, Nava A, Thiene G. Is arrhythmogenic right ventricular cardiomyopathy a paediatric problem too? *Images Paediatr Cardiol*. 2001;3:18–37.
44. Rustico MA, Benettoni A, Fontaliran F, Fontaine G. Prenatal echocardiographic appearance of arrhythmogenic right ventricle dysplasia: a case report. *Fetal Diagn Ther*. 2001;16:433–436. doi: 53954.
45. Wei L, Roberts W, Wang L, Yamada M, Zhang S, Zhao Z, Rivkees SA, Schwartz RJ, Imanaka-Yoshida K. Rho kinases play an obligatory role in vertebrate embryonic organogenesis. *Development*. 2001;128:2953–2962.
46. Zhao Z, Rivkees SA. Rho-associated kinases play an essential role in cardiac morphogenesis and cardiomyocyte proliferation. *Dev Dyn*. 2003;226:24–32. doi: 10.1002/dvdy.10212.
47. Knudsen KA, Soler AP, Johnson KR, Wheelock MJ. Interaction of alpha-actinin with the cadherin/catenin cell-cell adhesion complex via alpha-catenin. *J Cell Biol*. 1995;130:67–77.
48. Koitabashi N, Danner T, Zaiman AL, Pinto YM, Rowell J, Mankowski J, Zhang D, Nakamura T, Takimoto E, Kass DA. Pivotal role of cardiomyocyte TGF-β signaling in the murine pathological response to sustained pressure overload. *J Clin Invest*. 2011;121:2301–2312. doi: 10.1172/JCI44824.
49. Beffagna G, Occhi G, Nava A, Vitiello L, Ditadi A, Basso C, Bauce B, Carraro G, Thiene G, Towbin JA, Danieli GA, Rampazzo A. Regulatory mutations in transforming growth factor-beta3 gene cause arrhythmogenic right ventricular cardiomyopathy type 1. *Cardiovasc Res*. 2005;65:366–373. doi: 10.1016/j.cardiores.2004.10.005.
50. Irani RA, Xia Y. The functional role of the renin-angiotensin system in pregnancy and preeclampsia. *Placenta*. 2008;29:763–771. doi: 10.1016/j.placenta.2008.06.011.

Significance

Arrhythmogenic right ventricular cardiomyopathy (ARVC) is a genetically determined heart disease that is currently regarded as a disease of the cardiac desmosome. In this article, we suggest Rho-kinase as a new mediator in the development of ARVC. Using a novel mouse model, with Rho-kinase deficiency directed to the embryonic heart, we have demonstrated the development of a remarkable cardiac phenotype, recapitulating ARVC in humans. The cardiac desmosomal changes are of particular interest because they were not related to desmosomal gene mutations or over/underexpression, as in previous ARVC mouse models. We were also able to demonstrate a link between Rho-kinase deficiency and aberrant Wnt signaling, which has recently been implicated in the pathogenesis of ARVC. We think that Rho-kinase inhibition offers an explanation for the development of the seemingly unrelated cardiac changes observed in ARVC and justifies Rho-kinase as a novel target to be explored in ARVC.

Arteriosclerosis, Thrombosis, and Vascular Biology

JOURNAL OF THE AMERICAN HEART ASSOCIATION

Rho-Kinase Inhibition During Early Cardiac Development Causes Arrhythmogenic Right Ventricular Cardiomyopathy in Mice

Alia Ellawindy, Kimio Satoh, Shinichiro Sunamura, Nobuhiro Kikuchi, Kota Suzuki, Tatsuro Minami, Shohei Ikeda, Shinichi Tanaka, Toru Shimizu, Budbazar Enkhjargal, Satoshi Miyata, Yuhto Taguchi, Tetsuya Handoh, Kenta Kobayashi, Kazuto Kobayashi, Keiko Nakayama, Masahito Miura and Hiroaki Shimokawa

Arterioscler Thromb Vasc Biol. 2015;35:2172-2184; originally published online August 27, 2015;
doi: 10.1161/ATVBAHA.115.305872
Arteriosclerosis, Thrombosis, and Vascular Biology is published by the American Heart Association, 7272 Greenville Avenue, Dallas, TX 75231

Print ISSN: 1079-5642. Online ISSN: 1524-4636

SUPPLEMENTAL MATERIAL

Rho-kinase Inhibition during Early Cardiac Development Causes Arrhythmogenic Right Ventricular Cardiomyopathy in Mice

Alia Ellawindy,[1] Kimio Satoh,[1] Shinichiro Sunamura,[1] Nobuhiro Kikuchi,[1] Kota Suzuki,[1] Tatsuro Minami,[1,2] Shohei Ikeda,[1] Shin-ichi Tanaka,[1,2] Toru Shimizu,[1] Budbazar Enkhjargal,[1] Satoshi Miyata,[1] Yuhto Taguchi,[3] Tetsuya Handoh,[3] Kenta Kobayashi,[4] Kazuto Kobayashi,[4] Keiko Nakayama,[5] Masahito Miura,[3] Hiroaki Shimokawa[1]

[1]Department of Cardiovascular Medicine, Tohoku University Graduate School of Medicine, Sendai, Japan

[2]Laboratory for Pharmacology, Pharmaceuticals Research Center, Asahi Kasei Pharma Corporation, Izunokuni, Japan

[3]Department of Clinical Physiology, Health Science, Tohoku University Graduate School of Medicine, Sendai, Japan

[4]Department of Molecular Genetics, Institute of Biomedical Sciences, Fukushima Medical University School of Medicine, Fukushima, Japan

[5]United Centers for Advanced Research and Translational Medicine, Core Center of Cancer Research, Division of Cell Proliferation, Tohoku University Graduate School of Medicine, Sendai, Japan

Supplemental Tables I-II

Supplemental Figures I-XVII and its Figure Legends

Supplemental Figure Legends

Supplemental Figure I. Connexin43 in the Right Ventricles of DN-RhoK Mice
(**RV**) Immunofluorescence staining showing the distribution of Connexin43 in the right ventricle (RV) of DN-RhoK mice as compared with littermate controls (20 weeks). Note that the Connexin43 signal is situated at the myocardial cell-cell junction in control hearts, whereas the signal is significantly reduced in DN-RhoK hearts. (**LV**) Immunofluorescence staining showing the distribution of Connexin43 in the left ventricle (LV) of DN-RhoK mice as compared with littermate controls. Note that the Connexin43 signal is reduced in DN-RhoK hearts as compared with control hearts. Bar, 200 μm (×100), 50 μm (×400).

Supplemental Figure II. Hierarchical Clustering Analysis
Microarray analysis using the Agilent SurePrint G3 Mouse GE microarray kit revealed a significantly changed gene profiles in DN-RhoK hearts compared with age-matched controls (E12.5 embryonic hearts). All the relevant genes were grouped according to their expression values (log ratios). Each row corresponds to one gene, each column to the different 8 microarray experiments. The quantitative gene expression changes across all the samples are shown by different colors (red indicates up-regulated genes; green indicates down-regulated genes). The top labels indicate the different experiments.

Supplemental Figure III. Volcano Plots Analysis
The DN-RhoK hearts showed significant changes in 3,653 genes (1,909 increased; 1,744 decreased, $P<0.05$) as compared with the control hearts. Volcano plots analysis revealed the significantly altered gene expression profiles in DN-RhoK hearts. Significantly increased top 5 genes (DN-RhoK/control ratio>2.0, $P<0.05$) and significantly reduced top 16 genes (DN-RhoK/control ratio<0.5, $P<0.05$) are presented as a table.

Supplemental Figure IV. Heat Map Analysis
Heat map analysis showed that many genes are associated with the pathways of cell morphology, cellular assembly, cell-to-cell interaction, metabolism, connective tissue disorder and organismal development, all of which are related with the Rho-kinase signaling.
Red panels show the up-regulated genes in DN-RhoK hearts. Blue panels show the down-regulated genes in DN-RhoK hearts.

Supplemental Figure V. The RhoA Signaling in the Hearts of DN-RhoK Embryos
Using microarray, the gene expression profiles of the hearts of embryonic day (E) 12.5 DN-

RhoK embryos were compared with that of littermate controls. Genes are displayed in the network as nodes. The relationships among the genes are represented with lines according to the Ingenuity Pathway Analysis (IPA). Up-regulated and down-regulated genes in DN-RhoK mice compared with control mice are shown as red and green spots, respectively.

Supplemental Figure VI-XV. IPA Functional Analysis and Top 10 Networks Associated with Rho-kinase Inhibition in the Hearts of DN-RhoK Embryos

Using microarray, the gene expression profiles of the hearts of embryonic day (E) 12.5 DN-RhoK embryos were compared with that of littermate controls. Genes are displayed in the network as nodes. The relationships among the genes are represented with lines according to the Ingenuity Pathway Analysis (IPA) software. Up-regulated and down-regulated genes in DN-RhoK mice compared with control mice are shown as red and green spots, respectively.

Supplemental Figure VI.

No.1 Associated Network in DN-RhoK Cardiac Tissue: Molecular Transport, Drug Metabolism, Lipid Metabolism

Supplemental Figure VII.

No.2 Associated Network in DN-RhoK Cardiac Tissue: Cellular Compromise, Cell Cycle, Cellular Assembly and Organization

Supplemental Figure VIII.

No.3 Associated Network in DN-RhoK Cardiac Tissue: Cell Morphology, Cellular Movement, Digestive System Development and Function

Supplemental Figure IX.

No.4 Associated Network in DN-RhoK Cardiac Tissue: Connective Tissue Disorders, Developmental Disorder, Hereditary Disorder

Supplemental Figure X.

No.5 Associated Network in DN-RhoK Cardiac Tissue: RNA Post-Transcriptional Modification, Cell Morphology, Cellular Assembly and Organization

Supplemental Figure XI.

No.6 Associated Network in DN-RhoK Cardiac Tissue: Developmental Disorder,

Hematological Disease, Hereditary Disorder

Supplemental Figure XII.
No.7 Associated Network in DN-RhoK Cardiac Tissue: Molecular Transport, RNA Trafficking, Cancer

Supplemental Figure XIII.
No.8 Associated Network in DN-RhoK Cardiac Tissue: Cell Morphology, Cellular Assembly and Organization, Developmental Disorder

Supplemental Figure XIV.
No.9 Associated Network in DN-RhoK Cardiac Tissue: Protein Degradation, Protein Synthesis, Carbohydrate Metabolism

Supplemental Figure XV.
No.10 Associated Network in DN-RhoK Cardiac Tissue: Post-Translational Modification, DNA Replication, Recombination, and Repair, Organismal Development

Supplemental Figure XVI.
Representative Western blotting of Wnt5b, PPARγ, β-catenin, Plakoglobin.

Supplemental Figure XVII.
TUNEL assay showed a significant increase of apoptotic cells (shown as brown nuclei) in the postnatal hearts from DN-RhoK and control mice. Bar, 100 μm. Data are presented as the mean ± SEM. n=5 per group. *P<0.05 by Student's t test.

Supplemental Figure XVIII.
Relative gene expression of Axin2 signaling in embryonic day (E) 12.5 hearts and the right ventricle (RV) and left ventricle (LV) of 3-week-old mice. Relative expression levels are normalized to *Gapdh*. Data are presented as the mean ± SEM.

Supplemental Figure XIX.
Normal cardiac structure and function in mice with αMHC-directed DN-RhoK mice. (**A**) Normal heart morphology in mice with αMHC-directed DN-RhoK over-expression. Elastica-Masson staining of αMHC-directed DN-RhoK mice (αMHC-RhoK$^{+/-}$) and littermate controls (αMHC-RhoK$^{+/-}$) showed no signs of ARVC-like phenotype. Bar, 2 mm. (**B**)

Mean values of body weight (BW), heart weight (HW)/BW, right ventricular (RV) weight/BW and left ventricular (LV) weight/BW in 10-week-old mice. *n*=3 per group. Data are presented as the mean ± SEM. Student's *t* test showed no statistically significant differences between the 2 groups. (**C**) Echocardiographic parameters in 10-week-old mice with αMHC-directed DN-RhoK over-expression compared with littermate control mice, including interventricular septum thickness at end-diastole (IVSTd), LV end-systolic and end-diastolic diameters (LVESD and LVEDD, respectively), LV posterior wall diastolic thickness (LVPWTd), LV ejection fraction (LVEF) and fractional shortening (LVFS), and RV end-diastolic diameter (RVEDD). Data are presented as the mean ± SEM. *n*=3 per group. Student's *t* test showed no statistically significant differences between the 2 groups.

Supplemental Tables

Supplemental Table I. Primers and probes used for mouse genotyping and RT-PCR.

PCR primers for genotyping	
DN-RhoK-1	5’-ACT CAT CTC AGA AGA GGA TCT G-3’
DN-RhoK-2	5’-TTA GCT TGG CTT GTT TGG AGC-3’
IL-2 F	5’-CTA GGC CAC AGA ATT GAA AGA TCT-3’
IL-2 R	5’-GTA GGT GGA AAT TCT AGC ATC ATC C-3’
Cre-F	5’-GCG GTC TGG CAG TAA AAA CTA TC-3’
Cre-R	5’-GTG AAA CAG CAT TGC TGT CAC TT-3’
RT-PCR primers	
Ctnnb1-F	5’-CCT AGC TGG TGG ACT GCA GAA-3’
Ctnnb1-R	5’-CAC CAC TGG CCA GAA TGA TGA-3’
Wnt5b-F	5’-CTC TCA TGA ACC TAC AGA ACA ACG A-3’
Wnt5-R	5’-TGG AGC CAG CAG GTC TTG A-3’
Nppa-F	5’-TGA CAG GAT TGG AGC CCA GA-3’
Nppa-R	5’-GAC ACA CCA CAA GGG CTT AGG A-3’
Nppb-F	5’-AGC TGC TTT GGG CAC AAG ATA GA-3’
Nppb-R	5’-CCA GGC AGA GTC AGA AAC TGG AG-3’
Ctgf-F	5’-ACC CGA GTT ACC AAT GAC AAT ACC-3’
Ctgf-R	5’-CCG CAG AAC TTA GCC CTG TAT G-3’
Pparg-F	5’-TGT CGG TTT CAG AAG TGC CTT G-3’
Pparg-R	5’-TTC AGC TGG TCG ATA TCA CTG GAG-3’
Gapdh-F	5’-TGT GTC CGT CGT GGA TCT GA-3’
Gapdh-R	5’-TTG CTG TTG AAG TCG CAG GAG-3’
RT-PCR probes	
Rock1	5’-GGA GAC CTT CAA GCA CGA ATT ACA T-3’
Rock2	5’-GGT GTG AAC GGA TTT GGC CGT ATT G-3’
Gapdh	5’-GGT GTG AAC GGA TTT GGC CGT ATT G-3’

Supplemental Table II.

Top 25 Gene Networks Significantly Changed in DN-RhoK Hearts

No.	Top Diseases and Functions
1	Molecular Transport, Drug Metabolism, Lipid Metabolism
2	Cellular Compromise, Cell Cycle, Cellular Assembly and Organization
3	Cell Morphology, Cellular Movement, Digestive System Development and Function
4	Connective Tissue Disorders, Developmental Disorder, Hereditary Disorder
5	RNA Post-Transcriptional Modification, Cell Morphology, Cellular Assembly and Organization
6	Developmental Disorder, Hematological Disease, Hereditary Disorder
7	Molecular Transport, RNA Trafficking, Cancer
8	Cell Morphology, Cellular Assembly and Organization, Developmental Disorder
9	Protein Degradation, Protein Synthesis, Carbohydrate Metabolism
10	Post-Translational Modification, DNA Replication, Recombination, and Repair, Organismal Development
11	RNA Post-Transcriptional Modification, Infectious Disease, Organismal Injury and Abnormalities
12	Embryonic Development, Organismal Development, Tissue Development
13	DNA Replication, Recombination, and Repair, Energy Production, Nucleic Acid Metabolism
14	Cell Morphology, Connective Tissue Development and Function, Organismal Development
15	Amino Acid Metabolism, Post-Translational Modification, Small Molecule Biochemistry
16	Developmental Disorder, Hereditary Disorder, Metabolic Disease
17	Developmental Disorder, Hereditary Disorder, Neurological Disease
18	Amino Acid Metabolism, Small Molecule Biochemistry, Developmental Disorder
19	Embryonic Development, Tissue Development, Cell Cycle
20	Cellular Assembly and Organization, Cellular Function and Maintenance, Cell Cycle
21	Gene Expression, RNA Post-Transcriptional Modification, Respiratory Disease
22	RNA Post-Transcriptional Modification, Tissue Morphology, Carbohydrate Metabolism
23	Cancer, Cellular Assembly and Organization, Connective Tissue Development and Function
24	Developmental Disorder, Hereditary Disorder, Metabolic Disease
25	Gene Expression, DNA Replication, Recombination, and Repair, Dermatological Diseases and Conditions

Top 10 networks are shown in detail in the Supplementary Figures 8-17.

Supplemental Figure Ia

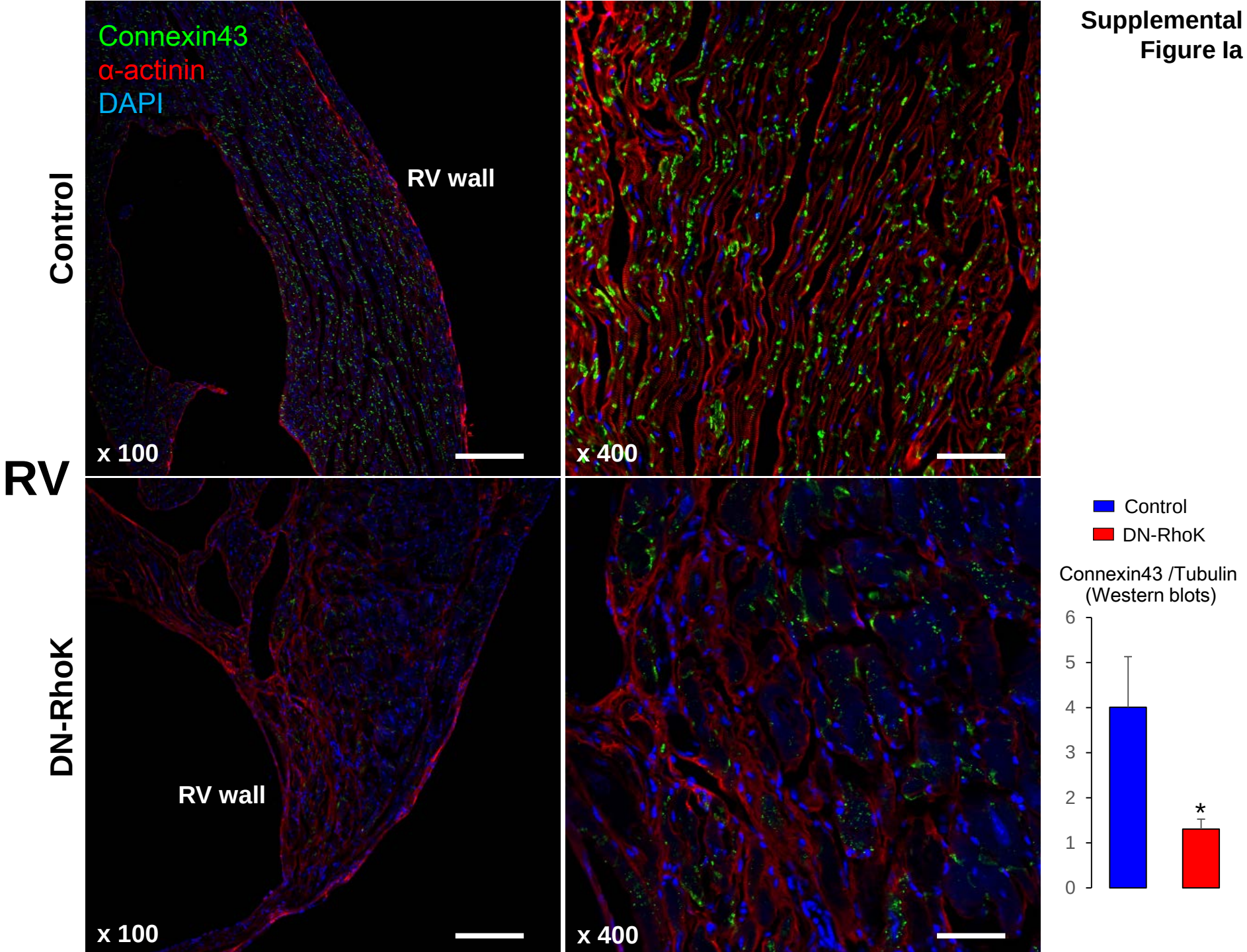

Supplemental Figure Ib

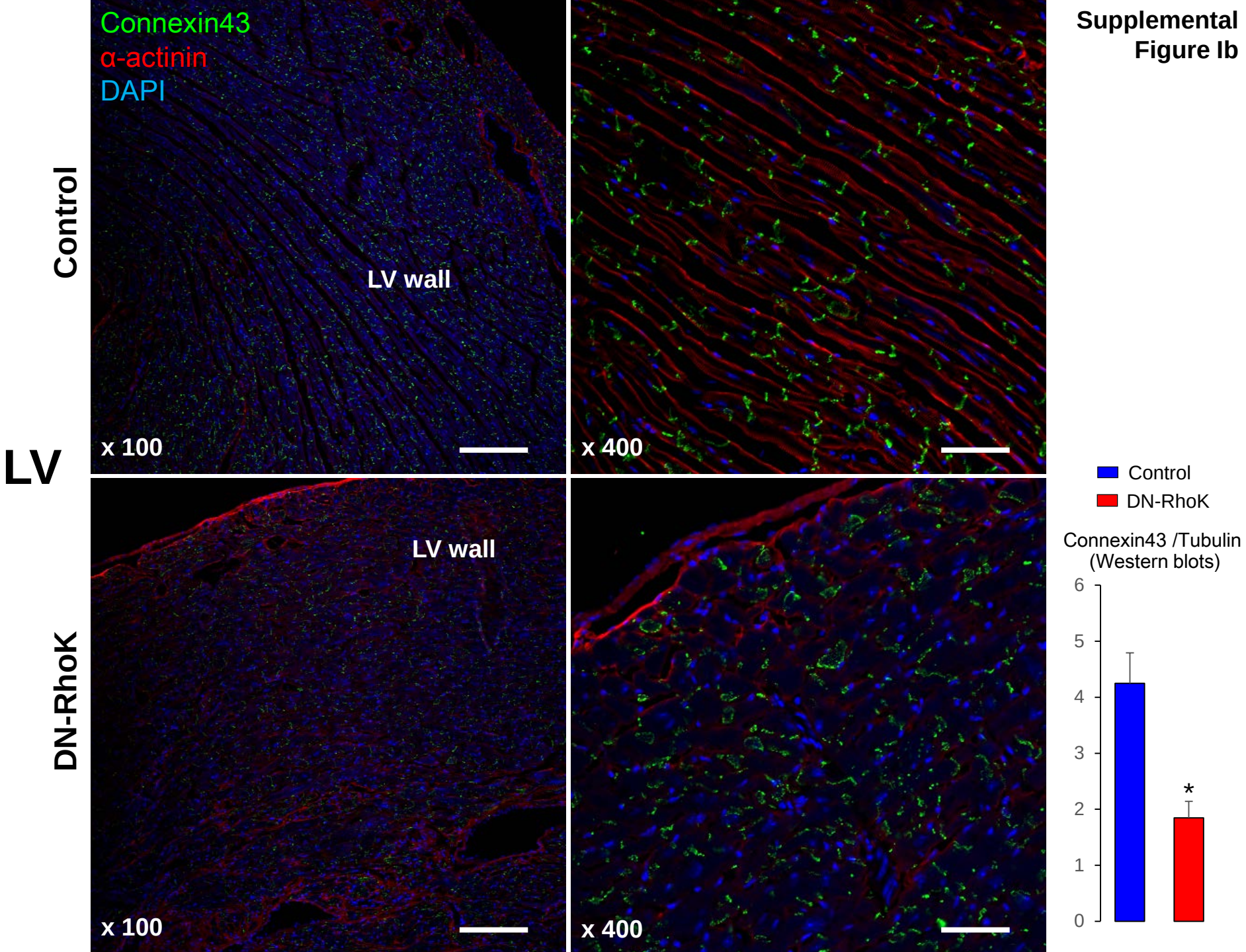

Hierarchical Clustering Analysis

Supplemental Figure II

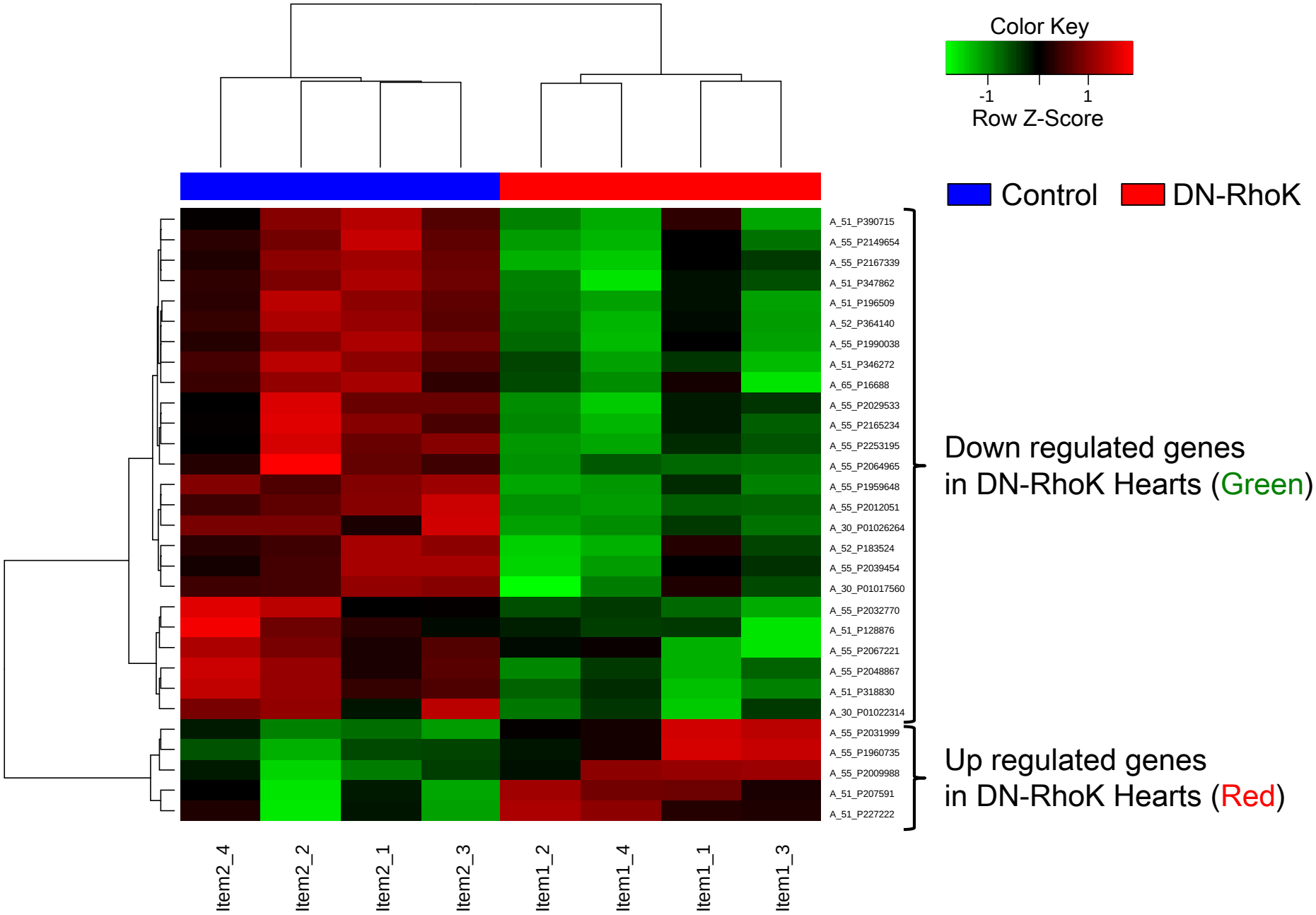

Supplemental Figure III

Volcano Plot Analysis

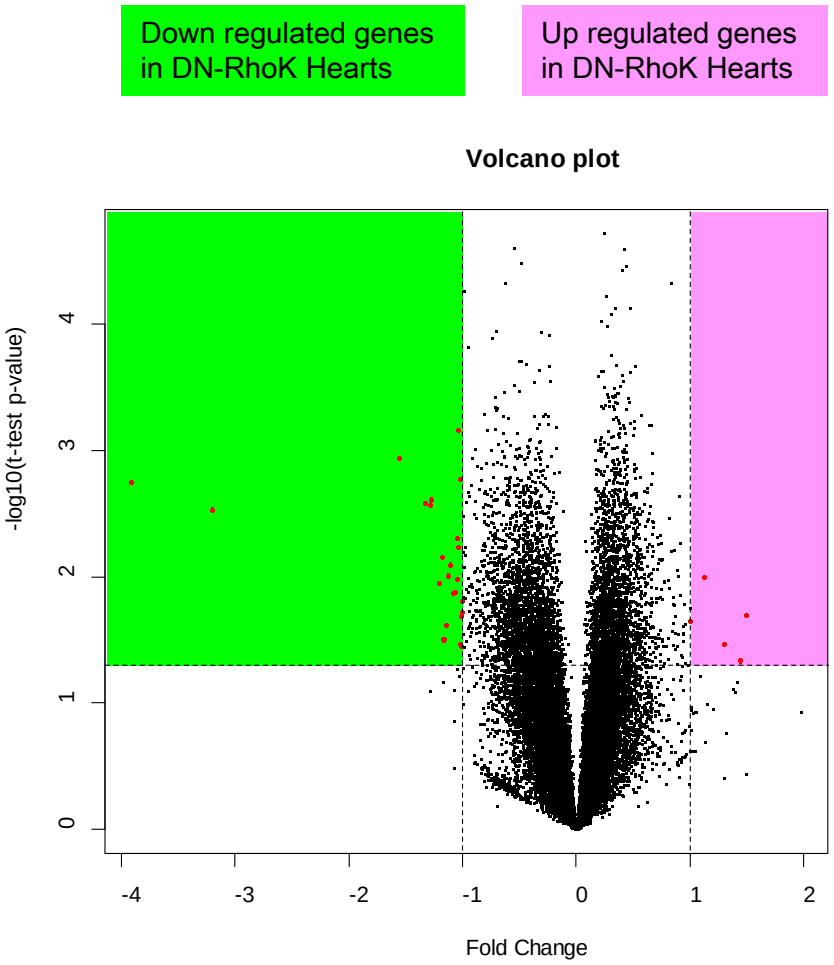

Symbol	Gene Name	p-value	DN-RhoK/WT (fold change)
C14orf159	chromosome 14 open reading frame 159	0.020	2.82
ADAMTS2	ADAM metallopeptidase with thrombospondin type 1 motif, 2	0.047	2.72
GDF15	growth differentiation factor 15	0.034	2.47
TRIB3	tribbles homolog 3 (Drosophila)	0.010	2.18
ANXA8L2	annexin A8-like 2	0.022	2.00
TAOK2	TAO kinase 2	0.019	0.50
TGFB1	transforming growth factor, beta 1	0.021	0.50
IFITM2	interferon induced transmembrane protein 2	0.036	0.49
ARHGAP33	Rho GTPase activating protein 33	0.002	0.49
HSPG2	heparan sulfate proteoglycan 2	0.001	0.49
DTX3	deltex homolog 3 (Drosophila)	0.006	0.49
MARK2	MAP/microtubule affinity-regulating kinase 2	0.005	0.48
CNOT3	CCR4-NOT transcription complex, subunit 3	0.011	0.48
ZFP57	ZFP57 zinc finger protein	0.013	0.48
TMEM86B	transmembrane protein 86B	0.024	0.45
INPP5E	inositol polyphosphate-5-phosphatase, 72 kDa	0.032	0.45
ACTN1	actinin, alpha 1	0.007	0.44
PLEKHJ1	pleckstrin homology domain containing, family J member 1	0.002	0.41
ITGA5	integrin, alpha 5 (fibronectin receptor, alpha polypeptide)	0.003	0.41
SOX1	SRY (sex determining region Y)-box 1	0.001	0.34
SYT10	synaptotagmin X	0.002	0.07

Heat Map Analysis

Supplemental Figure IV

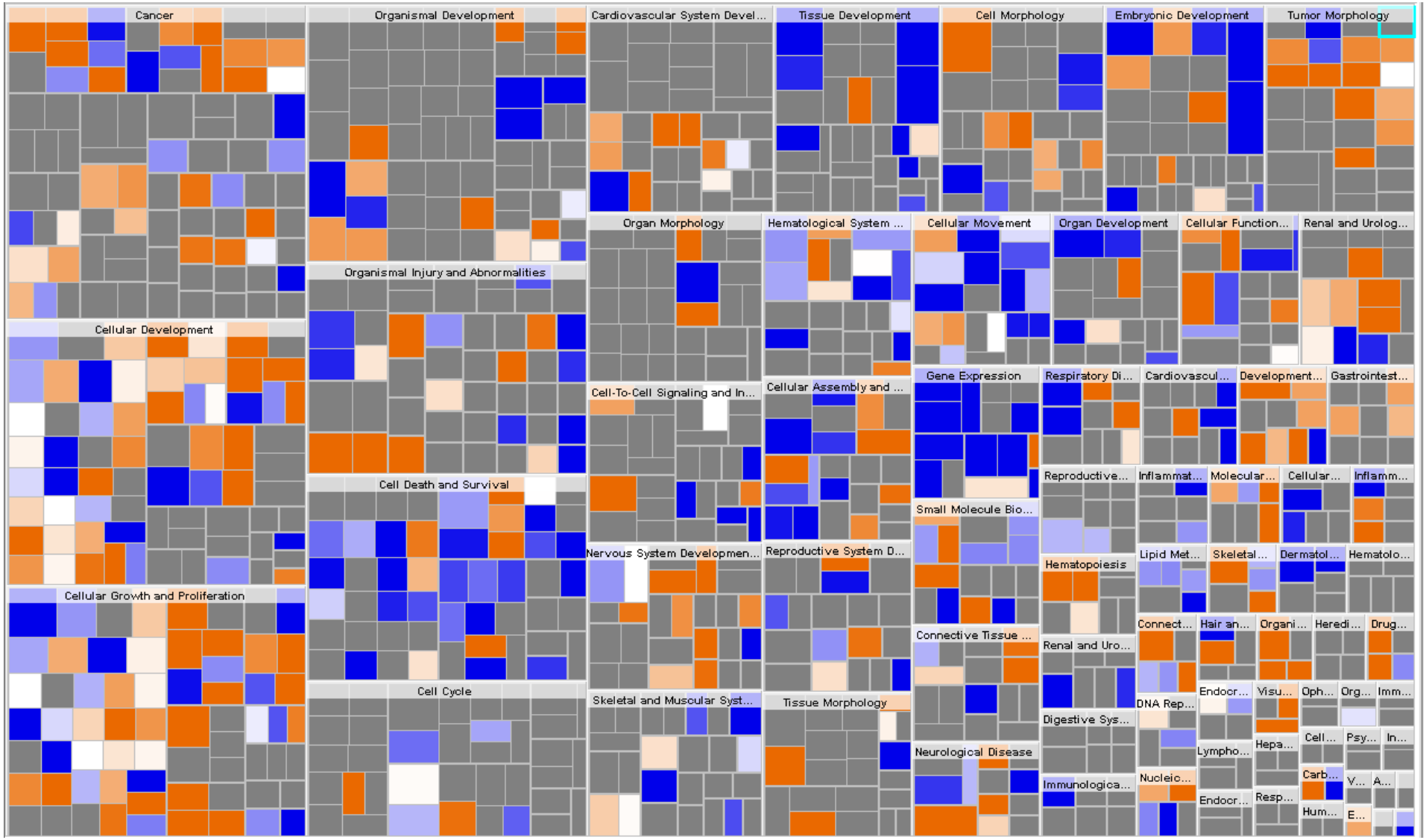

Down regulated genes in DN-RhoK Hearts

Up regulated genes in DN-RhoK Hearts

Changes in the RhoA/Rho-kinase Pathway in DN-RhoK Embryonic Heart

Supplemental Figure V

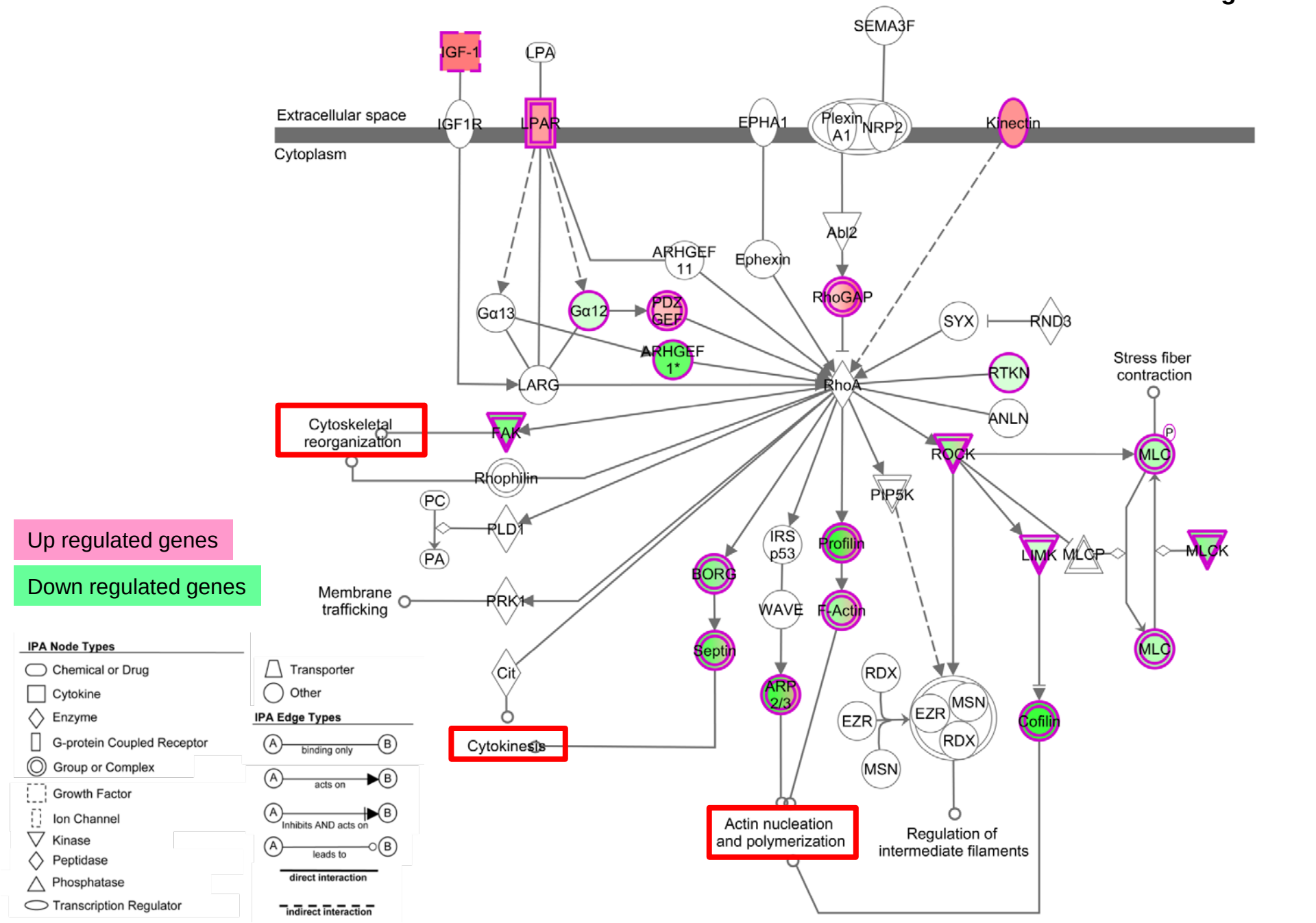

No.1 Associated Network in DN-RhoK Cardiac Tissue:

Molecular Transport, Drug Metabolism, Lipid Metabolism

Supplemental Figure VI

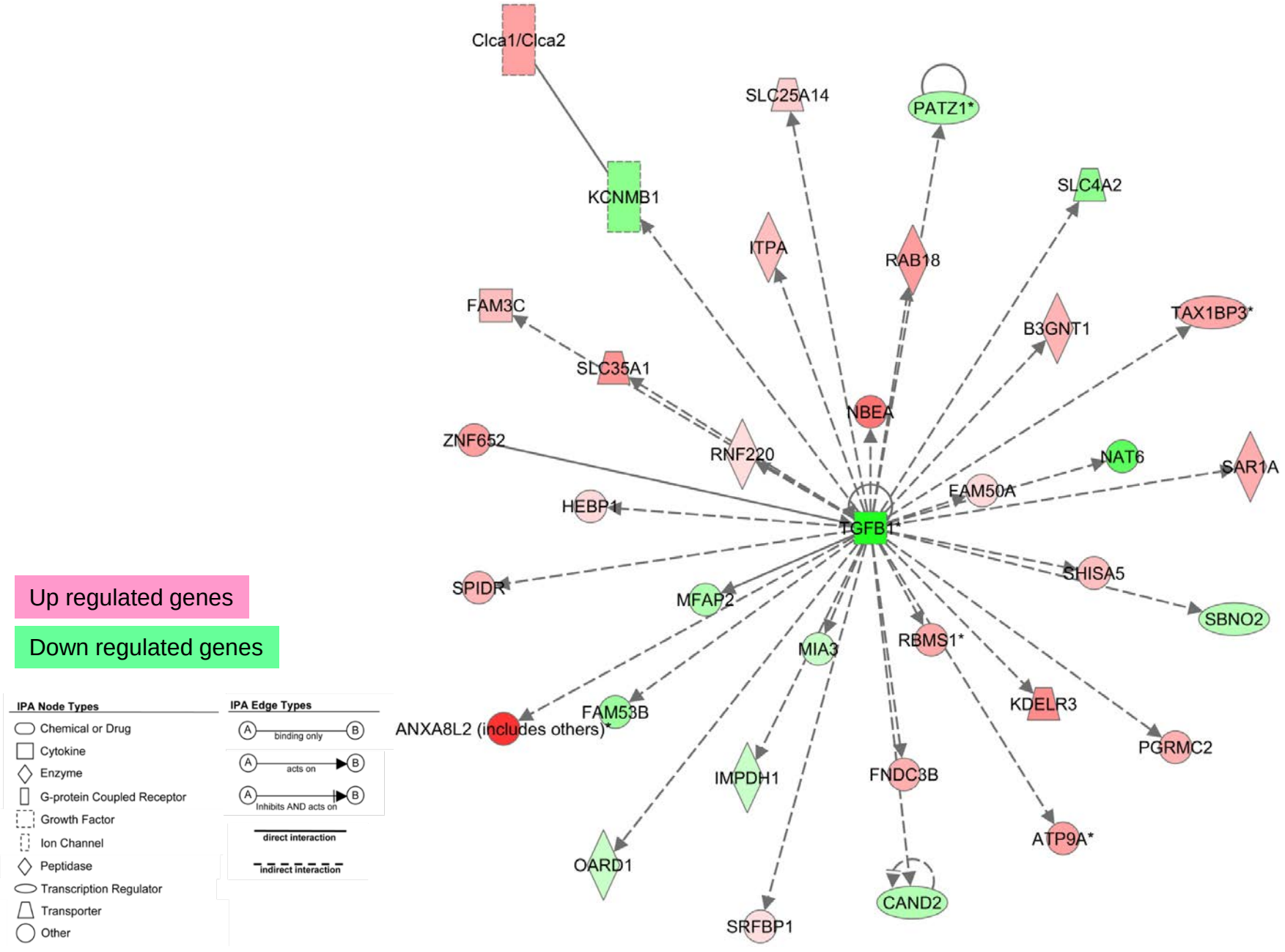

No.2 Associated Network in DN-RhoK Cardiac Tissue:

Cellular Compromise, Cell Cycle, Cellular Assembly and Organization

Supplemental Figure VII

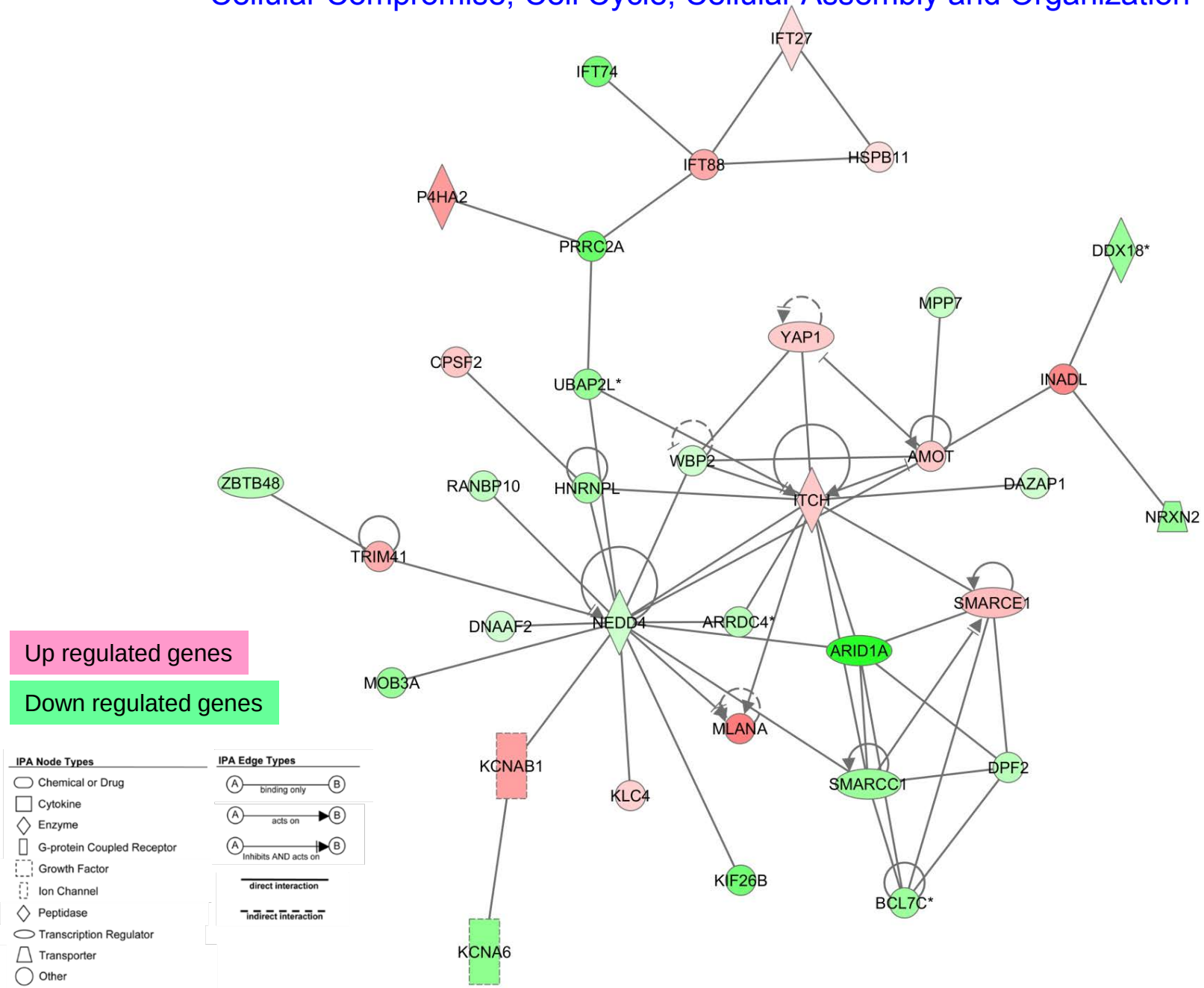

No.3 Associated Network in DN-RhoK Cardiac Tissue:

Cell Morphology, Cellular Movement, Digestive System Development and Function

Supplemental Figure VIII

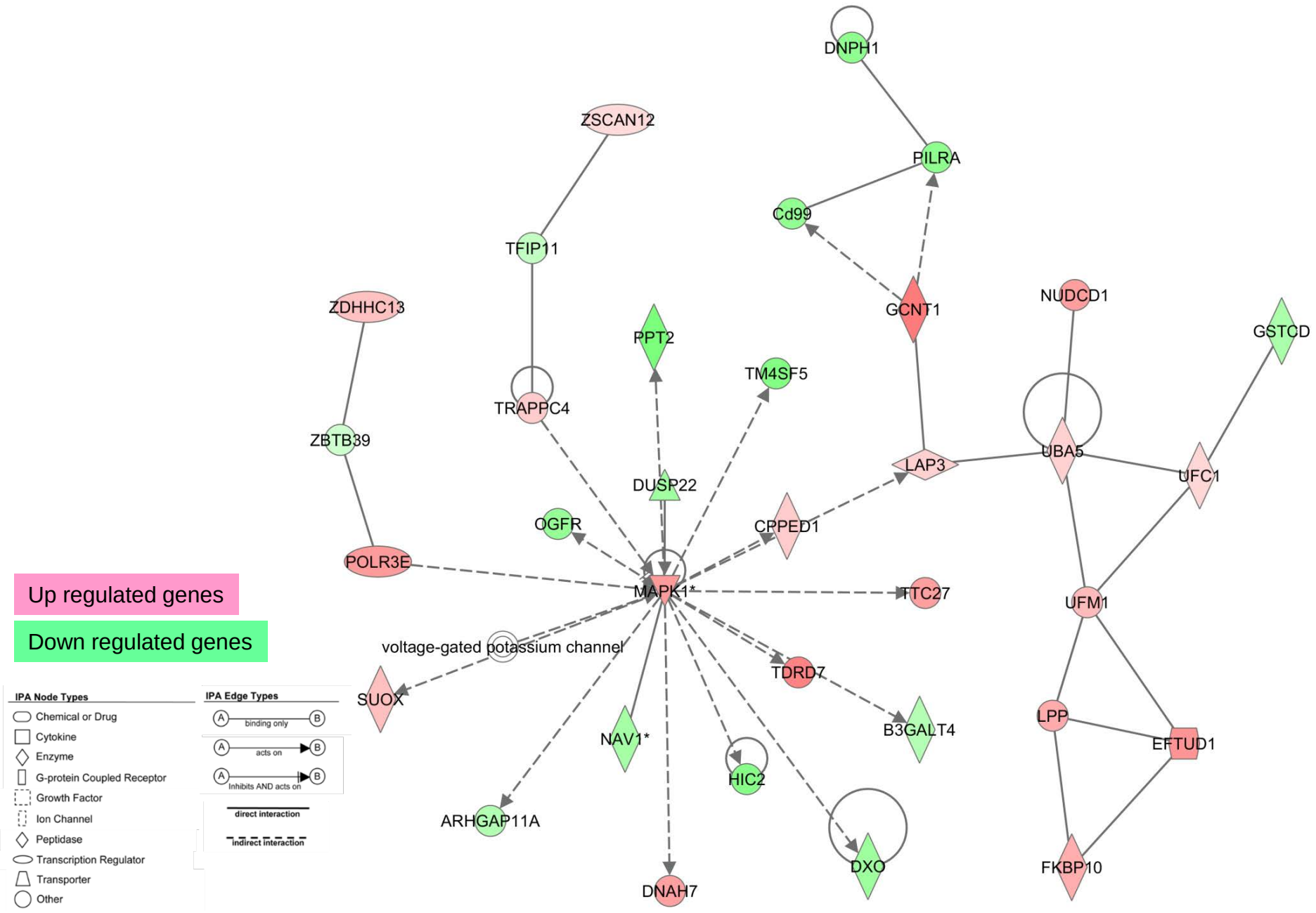

No.4 Associated Network in DN-RhoK Cardiac Tissue:

Connective Tissue Disorders, Developmental Disorder, Hereditary Disorder

Supplemental Figure IX

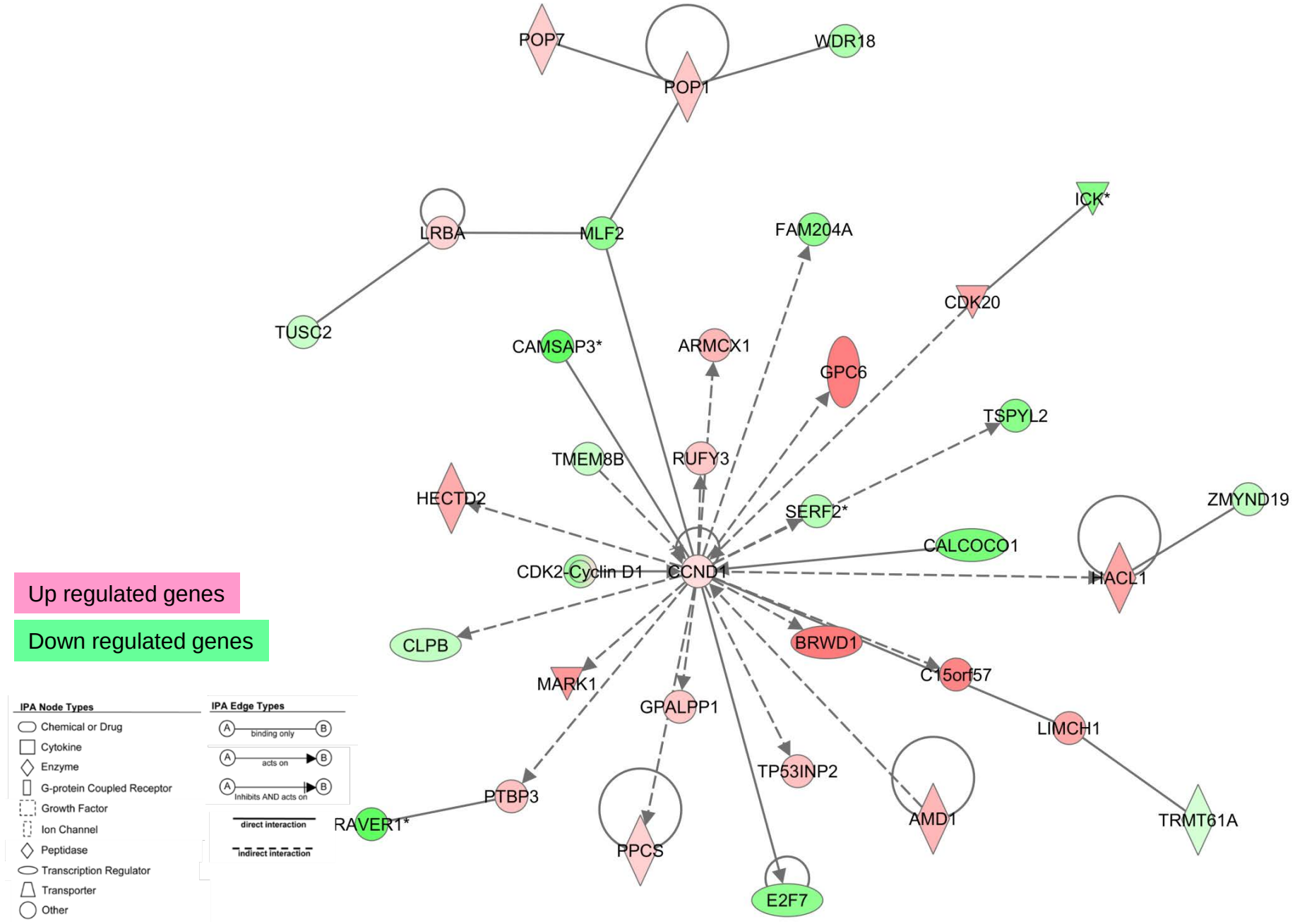

No.5 Associated Network in DN-RhoK Cardiac Tissue:

RNA Post-Transcriptional Modification, Cell Morphology, Cellular Assembly and Organization

Supplemental Figure X

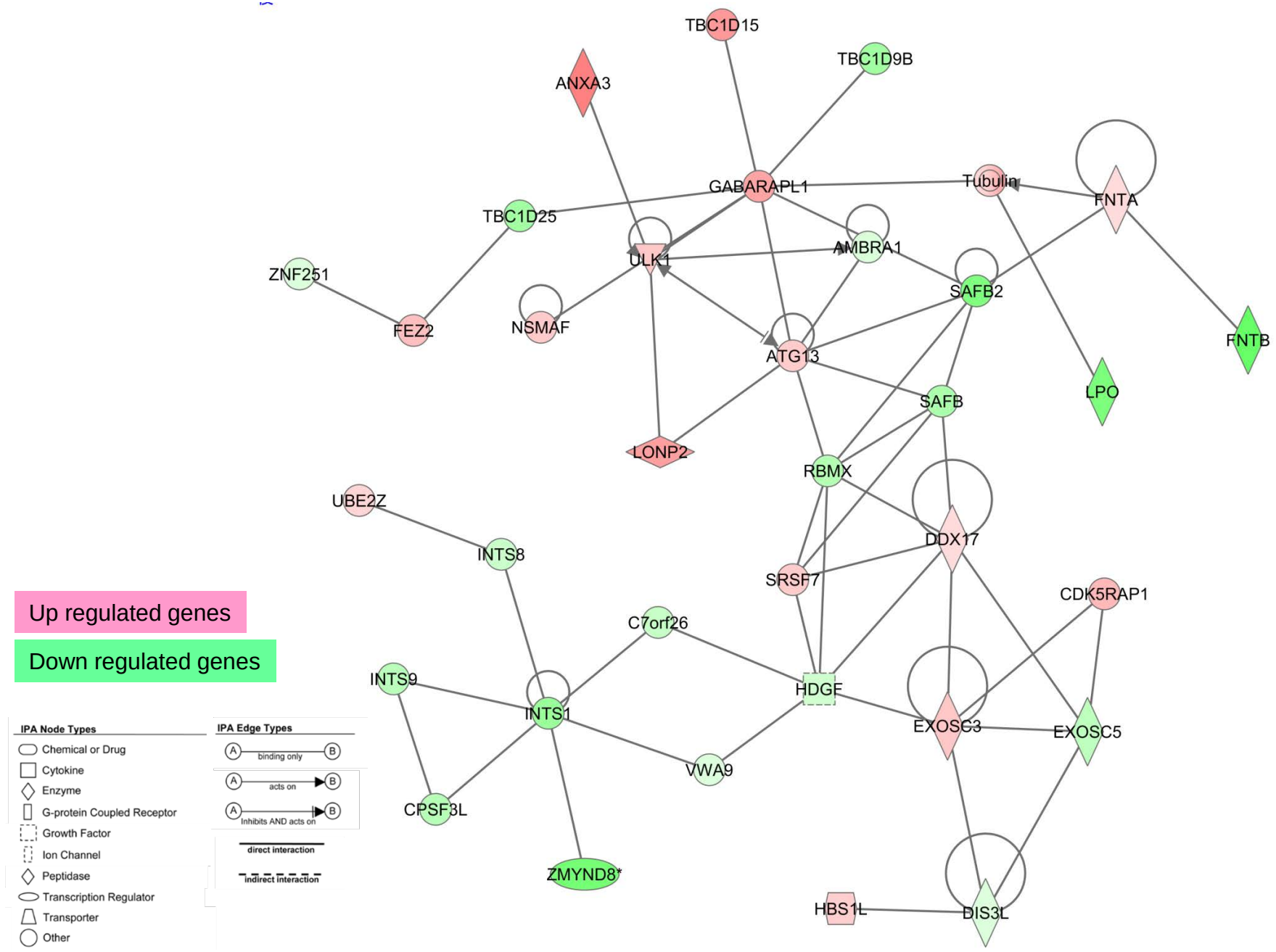

No.6 Associated Network in DN-RhoK Cardiac Tissue:

Developmental Disorder, Hematological Disease, Hereditary Disorder

Supplemental Figure XI

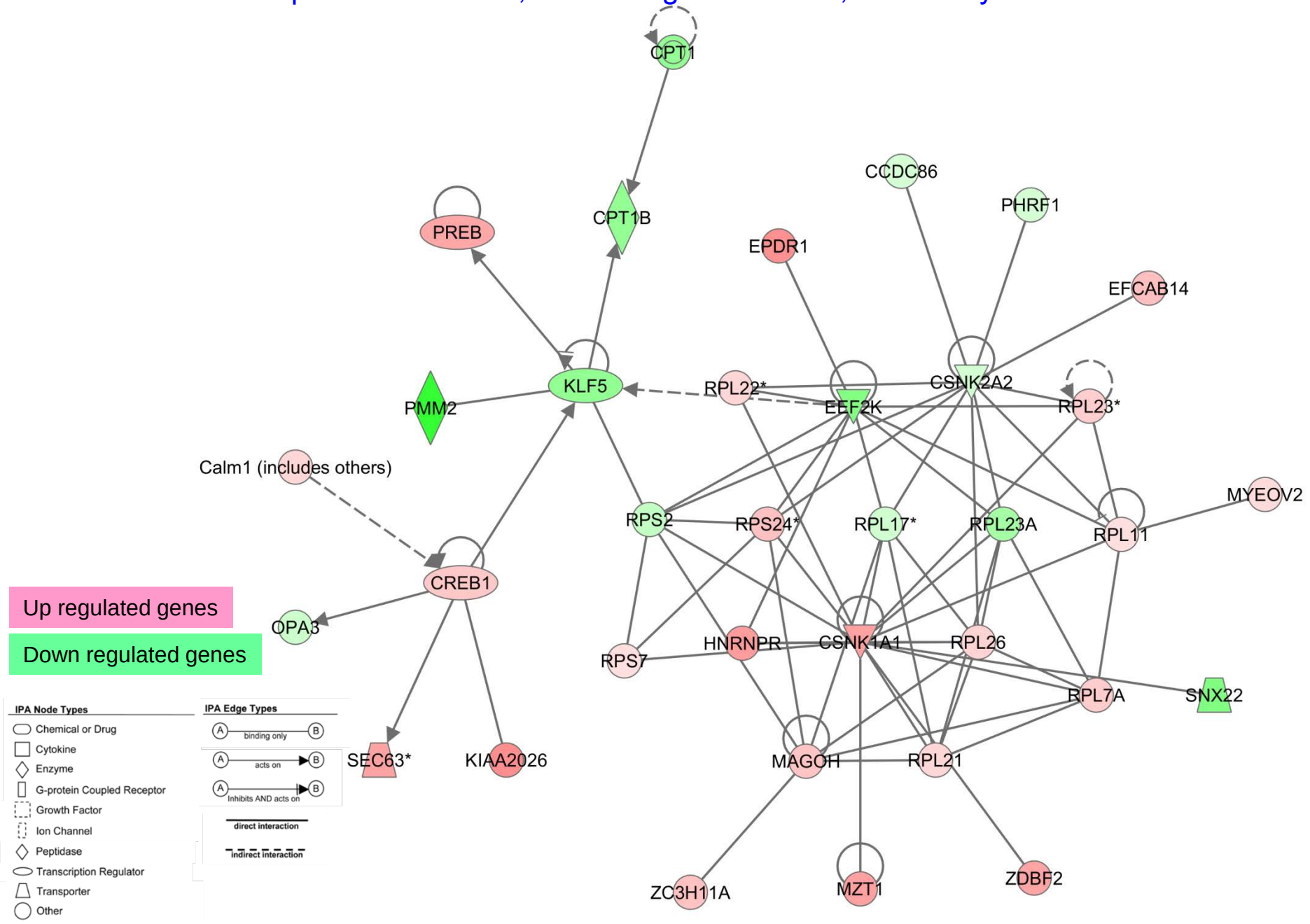

No.7 Associated Network in DN-RhoK Cardiac Tissue:

Molecular Transport, RNA Trafficking, Cancer

Supplemental Figure XII

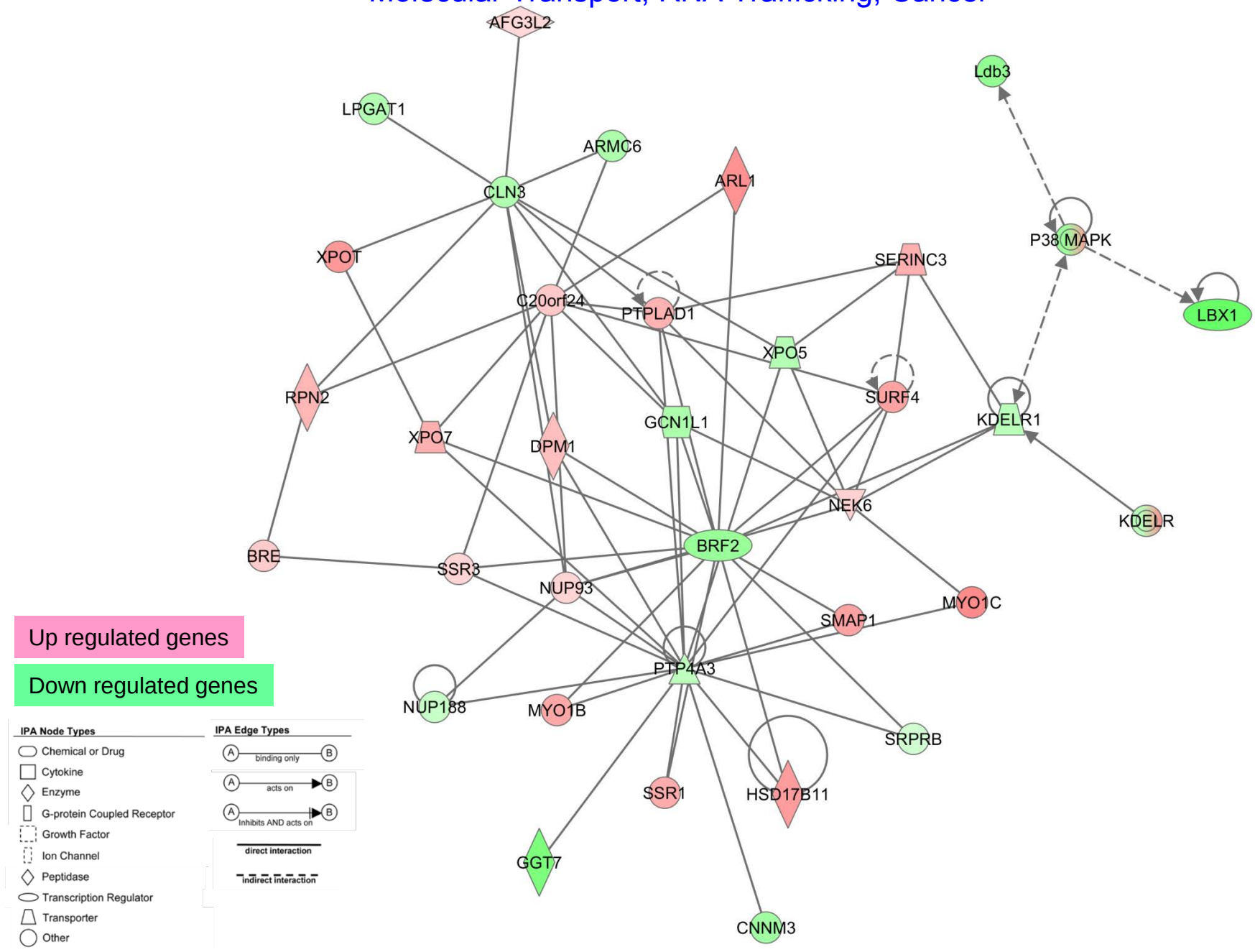

No.8 Associated Network in DN-RhoK Cardiac Tissue:

Cell Morphology, Cellular Assembly and Organization, Developmental Disorder

Supplemental Figure XIII

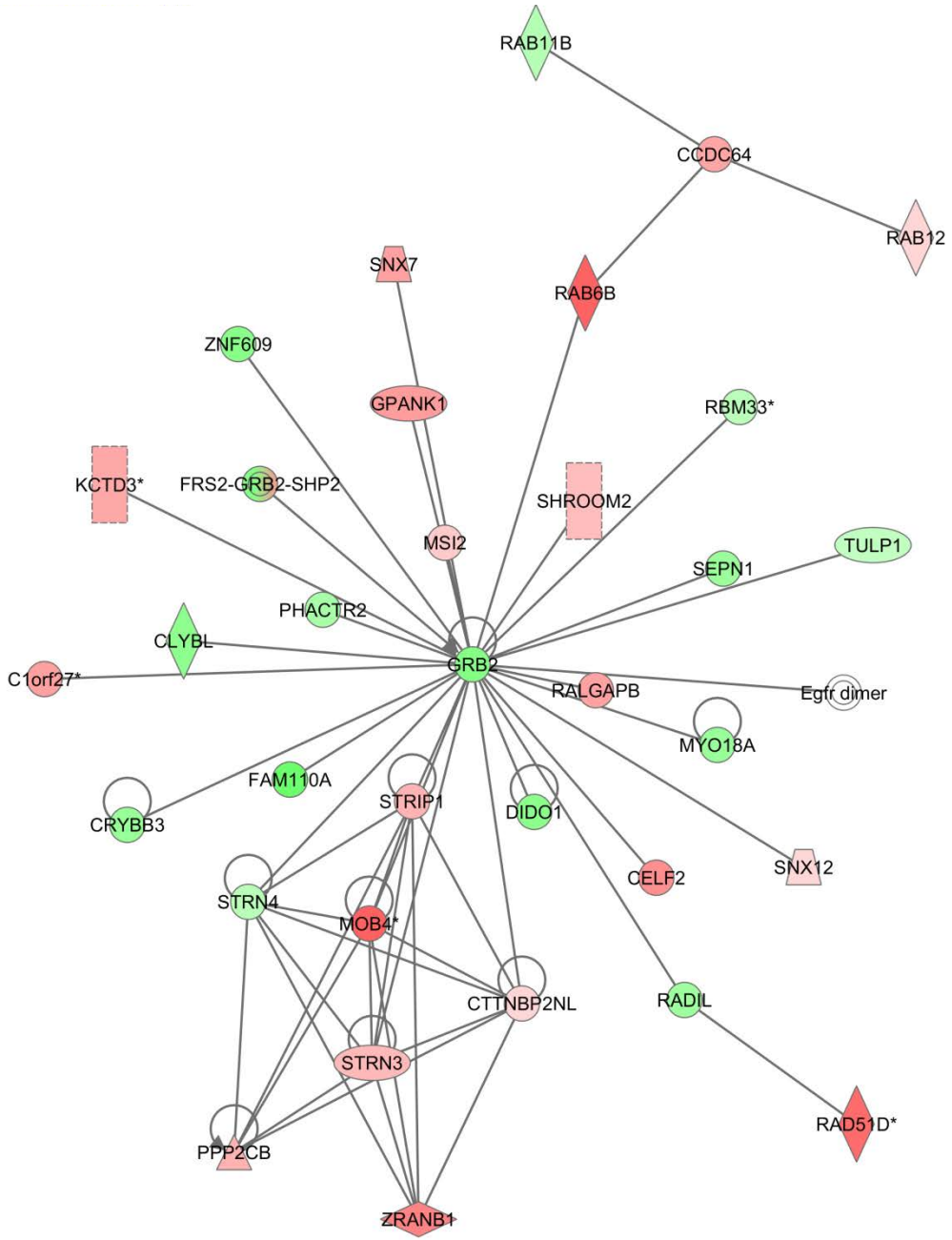

Up regulated genes

Down regulated genes

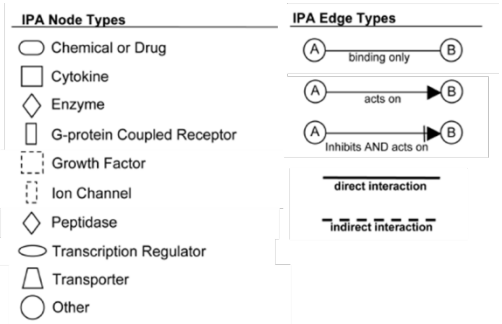

No.9 Associated Network in DN-RhoK Cardiac Tissue:
Protein Degradation, Protein Synthesis, Carbohydrate Metabolism

Supplemental Figure XIV

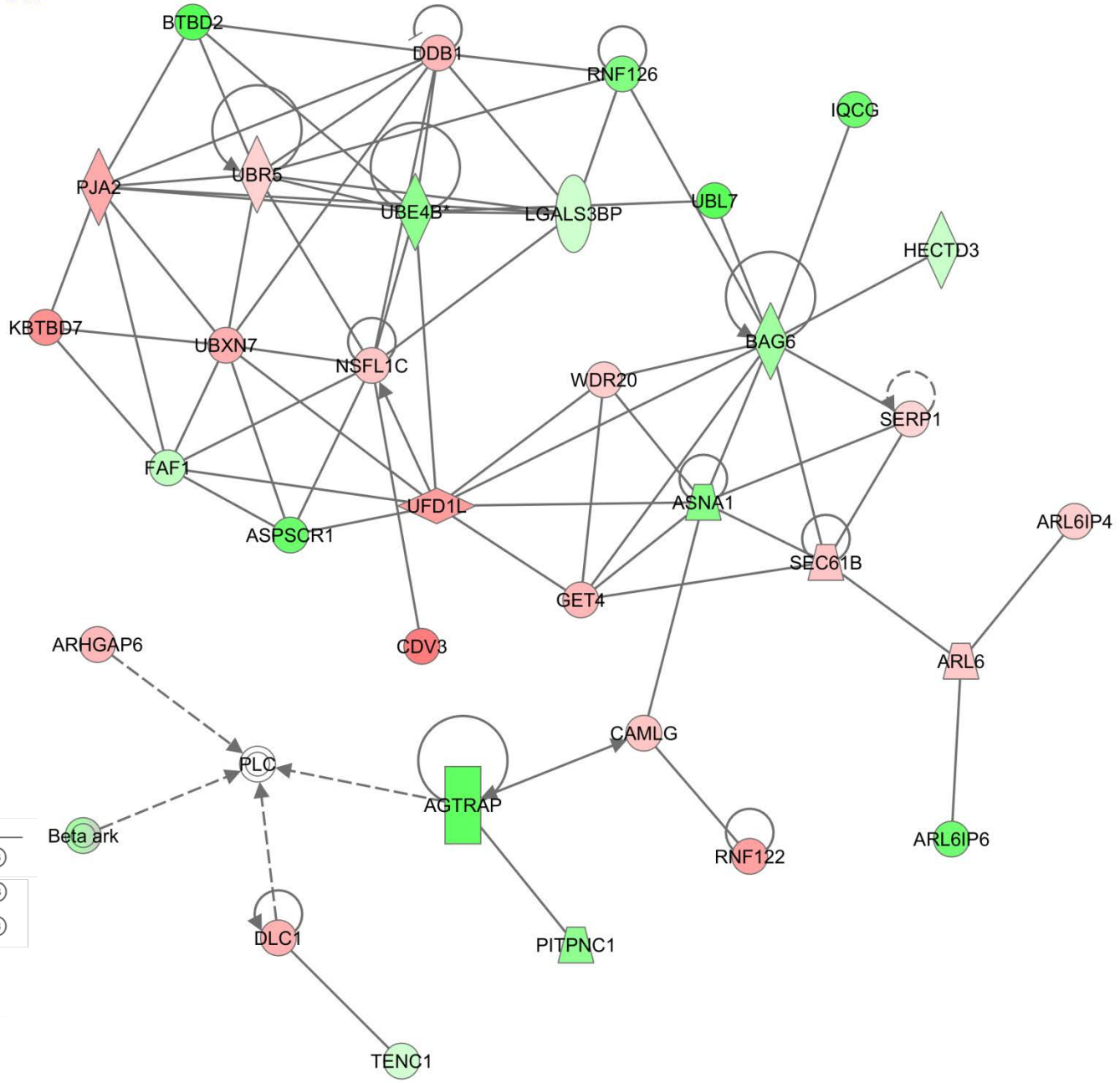

Up regulated genes

Down regulated genes

IPA Node Types

- Chemical or Drug
- Cytokine
- Enzyme
- G-protein Coupled Receptor
- Growth Factor
- Ion Channel
- Peptidase
- Transcription Regulator
- Transporter
- Other

IPA Edge Types

- binding only
- acts on
- Inhibits AND acts on
- direct interaction
- indirect interaction

No.10 Associated Network in DN-RhoK Cardiac Tissue:

Post-Translational Modification, DNA Replication, Recombination, and Repair, Organismal Development

Supplemental Figure XV

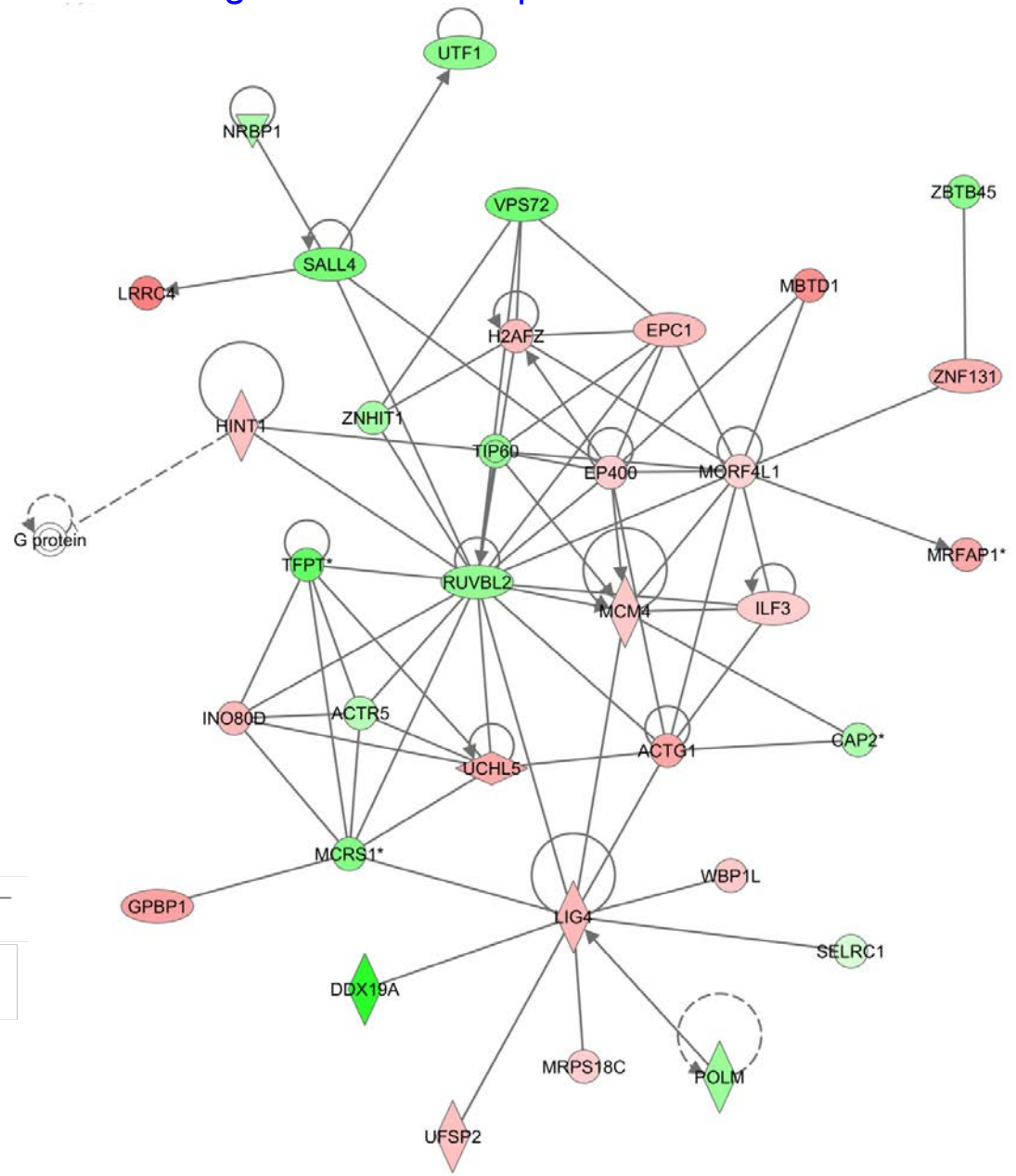

Up regulated genes

Down regulated genes

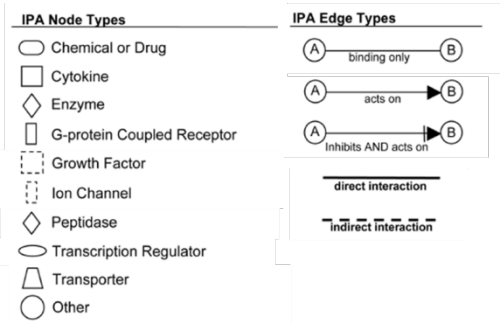

Supplemental Figure XVI

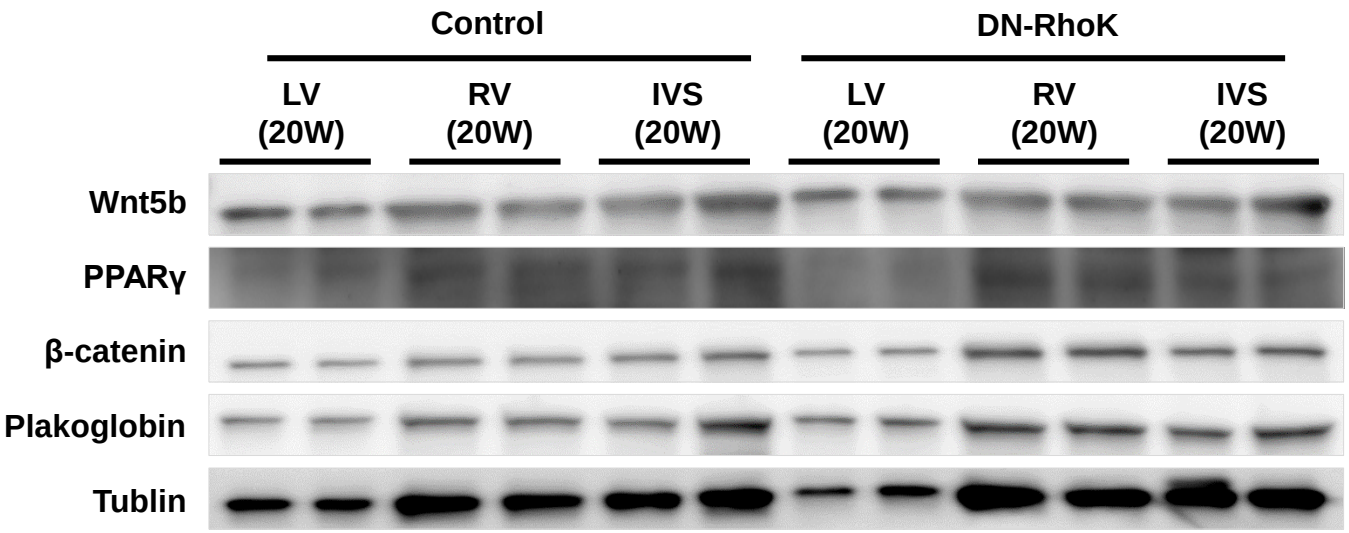

Supplemental Figure XVII

LV

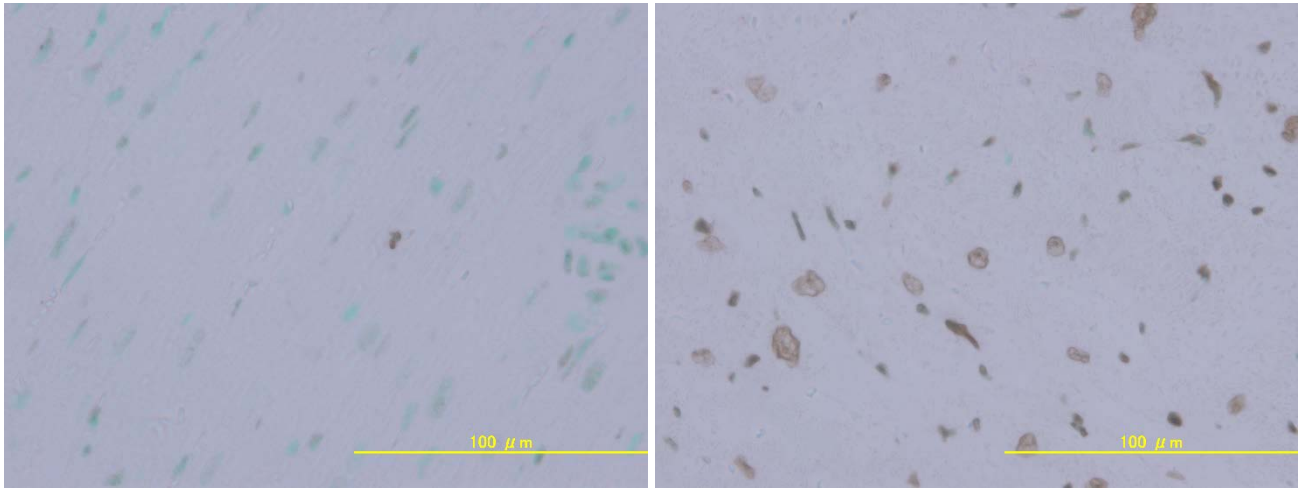

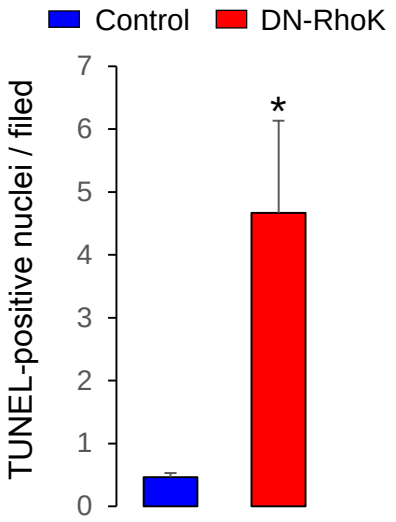

RV

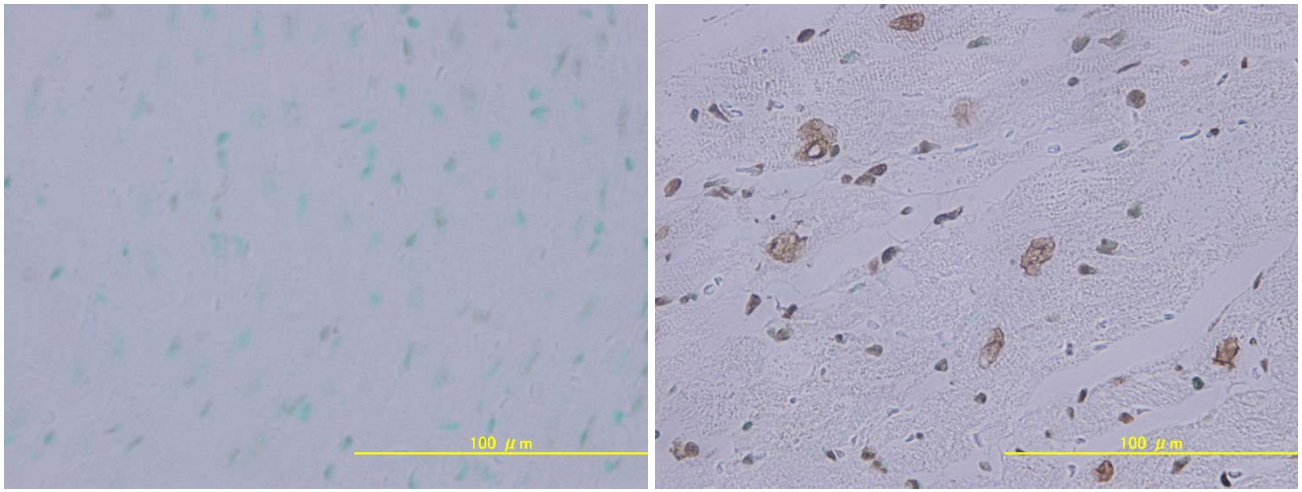

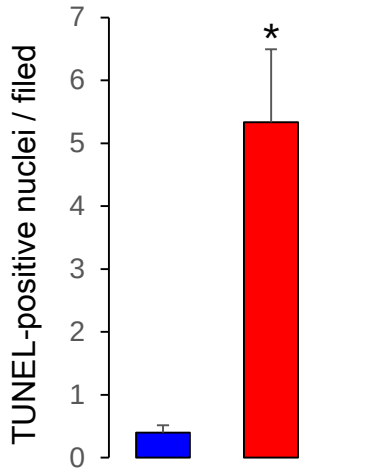

Supplemental Figure XVIII

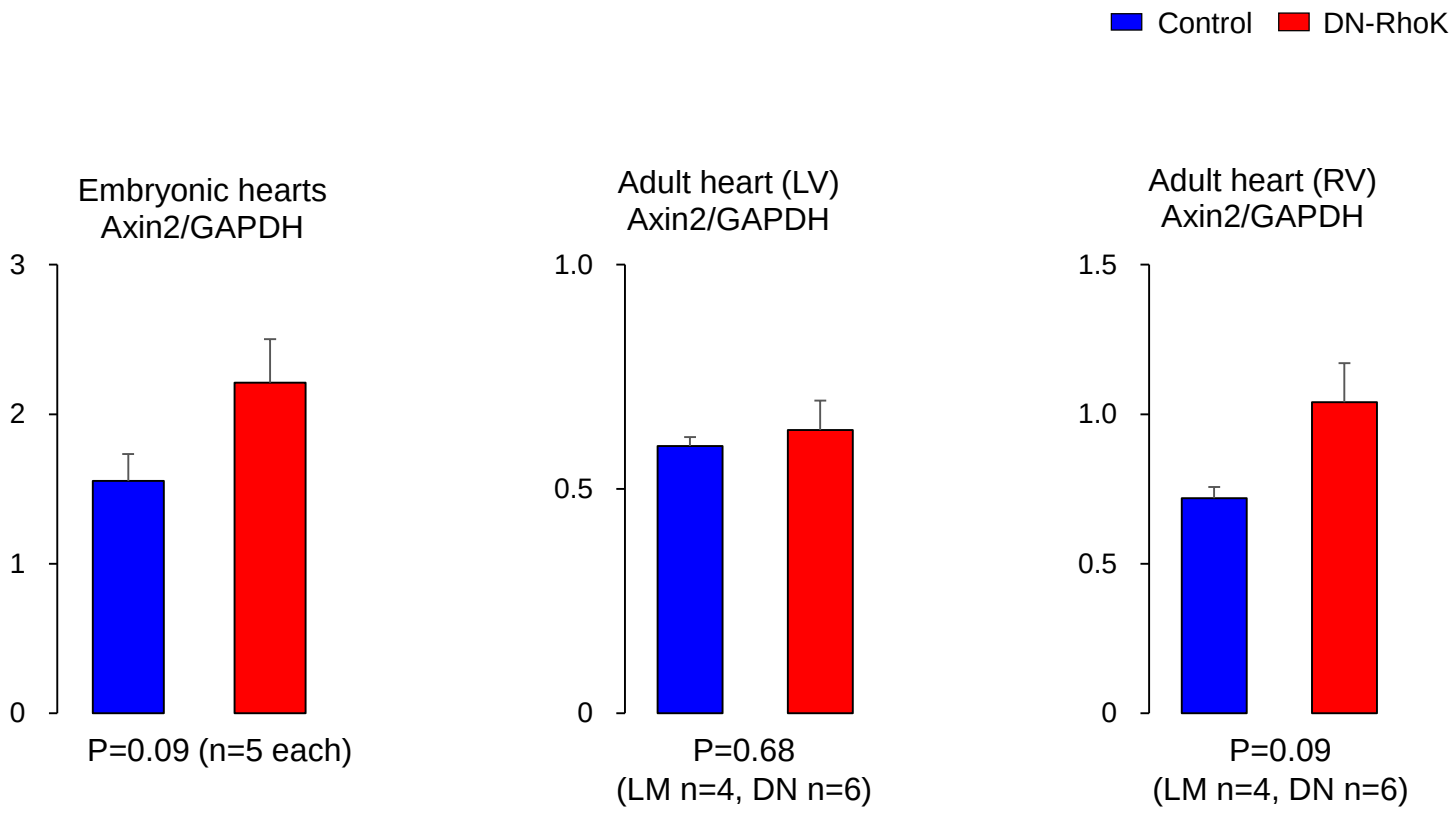

Supplemental Figure XIX

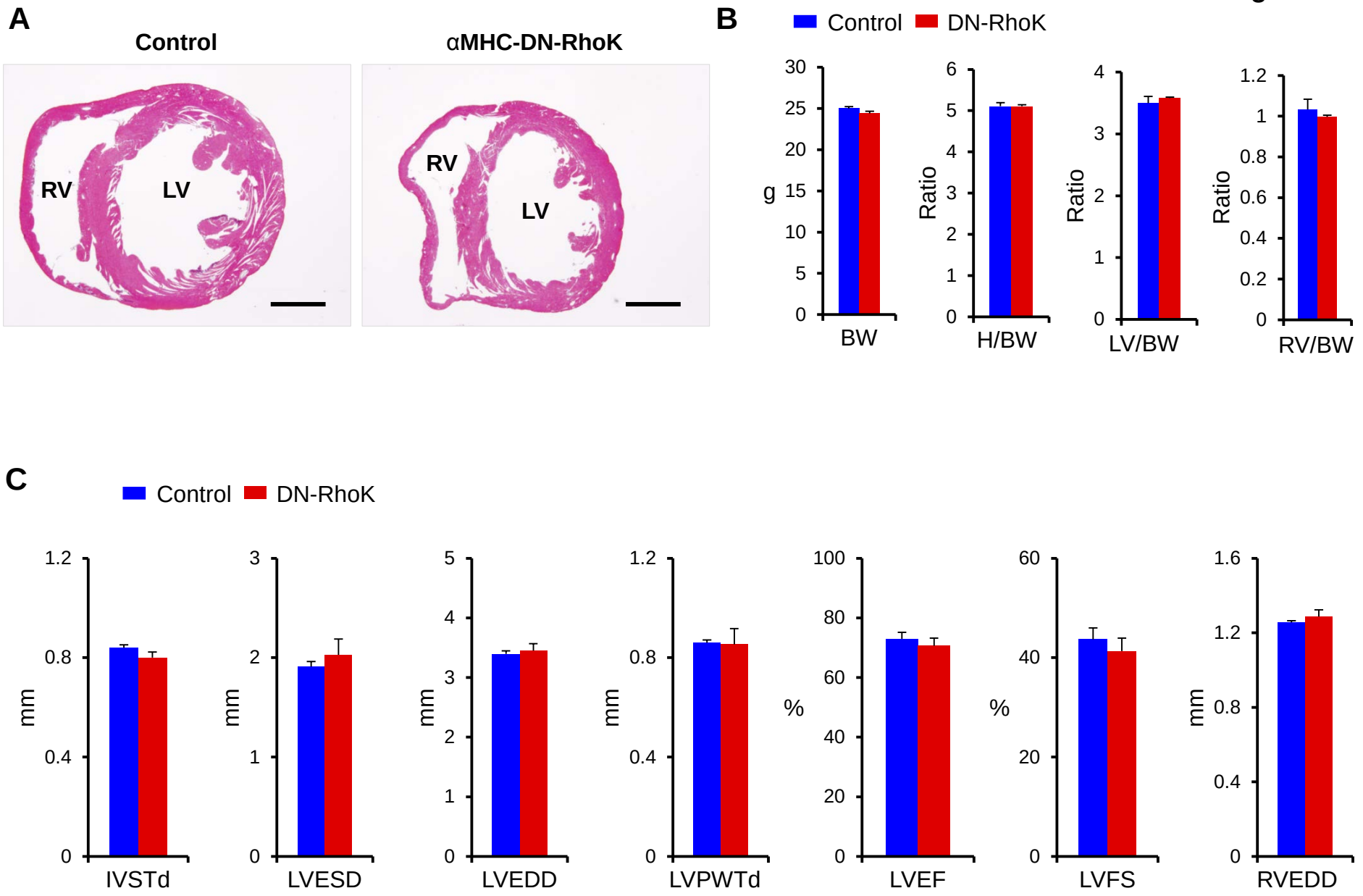

Materials and Methods

Transgenic Mice

All animal experiments were performed in accordance with the guidelines of the Tohoku University Ethics Committee on Animal Experiments (2012 Koudo-001). We used the SM22α promoter to target Rho-kinase activity during the development. Although SM22α is commonly known as a vascular smooth muscle cell-specific promoter, it has been increasingly used for cardiac muscle-selective expression as well.[1-3] SM22α is transiently expressed in the developing murine heart, starting in the heart field on E7.5,[4] making it a very early marker of the cardiovascular system. Importantly, once SM22α-Cre-promoter is activated, the switch of the Cre-loxP system continues to inhibit Rho-kinase in the heart. Interestingly, Rho-kinase expression is detectable in the murine heart from E7.5,[5] coinciding with the expression of SM22α. The SM22α (transgelin, *Tgln*) promoter was used to target DN-RhoK expression in the developing murine heart. Although SM22α is expressed in smooth muscle cells,[6] it is expressed in the developing mouse heart between embryonic days E7.5 and E12.5.[4, 6] Mice containing a dominant-negative Rho-kinase mutant (CAT-Rho-K DN/3-1, BRC_No 01294) were obtained from the Riken (Tsukuba, Japan). They were crossed with SM22α-Cre mice [Tg(Tagln-cre)1Her/J, Jackson Laboratory, Bar Harbor, U.S.A] or αMHC-Cre mice [Tg(Myh6-cre)1Jmk/J, Jackson Laboratory, Bar Harbor, U.S.A.] to obtain DN-RhoK mice (SM22α-Cre$^{+/-}$/DN-RhoK$^{+/-}$ and αMHC-Cre$^{+/-}$/DN-RhoK$^{+/-}$), respectively. Transgenic littermates lacking the DN-RhoK mutant (SM22α-Cre$^{+/-}$/DN-RhoK$^{-/-}$ and αMHC-Cre$^{+/-}$/DN-RhoK$^{-/-}$, respectively) were used as controls for all experiments. The genotype was confirmed by PCR amplification of tail DNA. The primers used are listed in the **Supplemental Table 1**.

Preparation of Mouse Embryos

Male SM22α-Cre mice were mated with female CAT-Rho-K DN/3-1 mice. For accurate timing of the pregnancy, female mice were examined the next morning for the presence of a vaginal plug. At noon on the day when vaginal plug was detected, the embryos were aged as embryonic day (E) 0.5. The pregnant mother was sacrificed by cervical dislocation and the embryos were dissected at noon on the 12th day (E12.5) and the 14th day (E14.5) after detection of the vaginal plug. Embryos were genotyped using DNA from tail biopsies.

Histology and Transmission Electron Microscopy (TEM)

Sections of paraffin-embedded whole embryos were examined by hematoxylin and eosin (H&E). The bromodeoxyuridine (5-bromo-2'-deoxy-uridine, *BrdU*) labeling and detection kit II (Roche, Basel, Switzerland) was used to examine cardiac cell proliferation in embryo sections. TUNEL assay was performed using the in situ apoptosis detection kit (Takara,

Otsu, Japan) to examine cardiac cell apoptosis in embryo sections. Paraffin sections of isolated post-natal hearts were examined with H&E, Masson and Elastica-Masson trichrome stains. Oil red O staining was used to detect adipogenic deposits in the heart. For TEM, isolated mouse hearts were fixed in 2% glutaraldehyde plus 2% paraformaldehyde/0.1 M phosphate buffered saline (pH 7.4) and processed for sectioning. TEM was performed with the aid of the electron microscopy laboratory of the Tohoku University Graduate School of Medicine, Sendai, Japan.

Echocardiography and Blood Pressure Measurements

Transthoracic echocardiography was performed using the Vevo 2100 system (Visualsonics, Toronto, Canada). Mice were anesthetized with isofluorane using 1.5% for induction and 1% for maintenance of anesthesia. Blood pressure was measured by the tail-cuff system (Muromachi Kikai Co., Ltd., MK-2000ST NP-NIBP Monitor, Tokyo, Japan) in conscious mice.

Telemetry ECG Monitoring

Mice were anesthetized with 1:1 pentobarbital (4 mg/ml) and xylasine hydroxychloride (5 mg/ml) in 0.1 ml/10 g body weight intraperitoneally. The telemetric ECG transmitter (Data Sciences International, TA10ETA-F20, St. Paul, USA) was implanted into the abdominal cavity with the electrodes placed subcutaneously, as previously described [7]. One week was allowed for convalescence after implantation. ECG was continuously recorded in freely mobile mice. Notocord-hem software (Notocord Systems S.A.S. Version 0.15, Croissy Sur Seine, France) was used for data acquisition.

Quantitative Real-Time PCR (qRT-PCR)

Total RNA was extracted from mouse hearts using the RNeasy Fibrous Tissue Mini Kit (Qiagen, Venlo, the Netherlands). Reverse transcription was performed using PrimeScript RT Master Mix (Perfect Real Time) (Takara, Otsu, Japan). qRT-PCR was performed using the CFX96 Real-Time System (BioRad, Hercules, USA), with both SYBR Green I and TaqMan gene expression assays. Relative expression levels were normalized to those of the house-keeping gene *Gapdh*. The primers used are listed in **Supplemental Table**.

Western Blot Analysis

Total protein was prepared from the aortas and the embryonic hearts of mice for Western blots using previously described protocols [8]. Briefly, proteins were separated via SDS-polyacrylamide gel electrophoresis and subsequently transferred to polyvinylidene difluoride (PVDF) membranes. Membranes were probed with primary antibodies against total (t) myosin phosphatase (MYPT) (BD Transduction Laboratories, 612165, Franklin Lakes, U.S.A.), phosphorylated (p) MYPT (Millipore, ABS45, Billerica, USA), α-tubulin (Sigma-

Aldrich, T5168, St. Louis, USA), and β-actin (Abcam, ab6276, Cambridge, UK). Rho-kinase activity was assessed by measuring the extent of phosphorylation of MYPT and was expressed as a relative blot density ratio, which was standardized to the positive control (PC) blot as (pMYPT sample density/tMYPT PC)/(tMYPT sample density/tMYPT PC density) [9].

Cell Protein Fractionation

Nuclear and membrane proteins were extracted from the ventricular tissues of mice using the Qproteome Cell Compartment Kit (Qiagen, Venlo, the Neatherlands). Proteins were used for Western blotting and the PVDF membranes were probed with primary antibodies against β-catenin (Sigma-Aldrich, C7082, St. Louis, USA). Membranes were stripped in WB Stripping Solution (Nacalai Tesque, Kyoto, Japan) and re-probed with antibodies against α-tubulin (Sigma-Aldrich, T5168, St. Louis, USA) and lamin A/C (BD Transduction Laboratories).

Immunofluorescence

The hearts were perfused with PBS and perfusion-fixed with 4% phosphate-buffered paraformaldehyde at physiological pressure for 5 min. The whole heart was harvested, fixed for 6 hours, embedded in OCT (Tissue-Tek, Miles Inc., Elkhart, Illinois, USA) and snap-frozen, and cross-sections (10 μm) were prepared. The sections were stained with primary antibodies for plakoglobin (γ-catenin; Santa Cruz Biotechnology, sc-7900, Dallas, USA), plakophilin 2 (Cat. No. 651167, Progen Biotechnik GmbH, Heidelberg, Germany), desmoglein 1+2 (Cat. No. 61002, Progen Biotechnik GmbH, Heidelberg, Germany), α-actinin (Abcam, ab9465, Cambridge, UK), β-catenin (Sigma-Aldrich, C7082, St. Louis, USA), and actin (Santa Cruz Biotechnology, sc-1616, Dallas, USA). The secondary antibodies used were Alexa Fluor® 488 goat anti-rabbit IgG (H+L) antibody (Life Technologies, A-11008, Carlsbad, California, USA) and Alexa Fluor® 594 goat anti-mouse IgG (H+L) antibody (Life Technologies, A-11005, Carlsbad, California, USA). The sections were mounted with ProLong® Gold Antifade Reagent with DAPI (Life Technologies, P-36931, Carlsbad, California, USA) and examined under fluorescence microscopy.

Microarray

RNA was extracted from the whole heart of E12.5 mouse embryo and was quantified using NanoDrop 2000C (Thermo Scientific, Wilmington, USA). For microarray expression profiling, samples (n=4 in each group) were processed using the Agilent SurePrint G3 Mouse GE Microarray Kit (Agilent Technologies, G4852A Palo Alto, USA). The statistical computing software R (version 3.0.2.) was used for preprocessing and statistical analysis. Differentially expressed genes were considered significant at P values of <0.05. Genes with significant changes were further subjected to pathway analysis using Ingenuity Pathway Analysis (IPA) (http://www.ingenuity.com) to identify gene sets representing specific

biological processes or functions.

Statistical Analysis

The log-rank test was used to determine the P value for Kaplan-Meier survival curves. Other data were presented as mean ± SEM. Student's t test was used to calculate the P values. P values of <0.05 were considered to be statistically significant.

References

1. Umans L, Cox L, Tjwa M, Bito V, Vermeire L, Laperre K, Sipido K, Moons L, Huylebroeck D and Zwijsen A. Inactivation of Smad5 in endothelial cells and smooth muscle cells demonstrates that Smad5 is required for cardiac homeostasis. *Am J Pathol*. 2007;170: 1460-1472.

2. El-Bizri N, Guignabert C, Wang L, Cheng A, Stankunas K, Chang CP, Mishina Y and Rabinovitch M. SM22alpha-targeted deletion of bone morphogenetic protein receptor 1A in mice impairs cardiac and vascular development, and influences organogenesis. *Development*. 2008;135:2981-2991.

3. Yoshida T, Gan Q, Franke AS, Ho R, Zhang J, Chen YE, Hayashi M, Majesky MW, Somlyo AV and Owens GK. Smooth and cardiac muscle-selective knock-out of Kruppel-like factor 4 causes postnatal death and growth retardation. *J Biol Chem*. 2010;285:21175-21184.

4. Yang M, Jiang H and Li L. Sm22alpha transcription occurs at the early onset of the cardiovascular system and the intron 1 is dispensable for its transcription in smooth muscle cells during mouse development. *Int J Physiol Pathophysiol Pharmacol*. 2010;2:12-19.

5. Wei L, Roberts W, Wang L, Yamada M, Zhang S, Zhao Z, Rivkees SA, Schwartz RJ and Imanaka-Yoshida K. Rho kinases play an obligatory role in vertebrate embryonic organogenesis. *Development*. 2001;128:2953-2962.

6. Li L, Miano JM, Cserjesi P and Olson EN. SM22 alpha, a marker of adult smooth muscle, is expressed in multiple myogenic lineages during embryogenesis. *Circ Res*. 1996;78:188-195.

7. Kramer K, van Acker SABE, Voss H-P, Grimbergen JA, van der Vijgh WJF and Bast A. Use of telemetry to record electrocardiogram and heart rate in freely moving mice. *Journal of Pharmacological and Toxicological Methods*. 1993;30:209-215.

8. Liu PY and Liao JK. A method for measuring Rho kinase activity in tissues and cells. *Methods Enzymol*. 2008;439:181-189.

9. Abe K, Shimokawa H, Morikawa K, Uwatoku T, Oi K, Matsumoto Y, Hattori T, Nakashima Y, Kaibuchi K, Sueishi K and Takeshit A. Long-term treatment with a Rho-kinase inhibitor improves monocrotaline-induced fatal pulmonary hypertension in rats. *Circ Res*. 2004;94:385-393.